Developmental And Comparative Immunology
July 2018, Volume 84 Pages 48-61
https://doi.org/10.1016/j.dci.2018.01.013
https://archimer.ifremer.fr/doc/00440/55139/

Archimer
https://archimer.ifremer.fr

Oestrogen, an evolutionary conserved regulator of T cell differentiation and immune tolerance in jawed vertebrates?

Paiola Matthieu [1], Knigge Thomas [1], Duflot Aurelie [1], Pinto Patricia I. S. [2], Farcy Emilie [3], Monsinjon Tiphaine [1, *]

[1] Univ Le Havre, Normandy Univ, FR CNRS SCALE 3730, UMR I INERIS URCA ULH Environm Stress & Aquat Bio, F-76600 Le Havre, France.
[2] Univ Algarve, CCMAR Ctr Marine Sci, Lab Comparat Endocrinol & Integrat Biol, P-8005139 Faro, Portugal.
[3] Montpellier Univ, UMR MARBEC, UM, CNRS,Ifremer,IRD, F-34095 Montpellier, France.

* Corresponding author : Tiphaine Monsinjon, email address : tiphaine.monsinjon@unlv-lehavre.fr

Abstract :

In teleosts, as in mammals, the immune system is tightly regulated by sexual steroid hormones, such as oestrogens. We investigated the effects of 17 beta-oestradiol on the expression of several genes related to T cell development and resulting T cell subpopulations in sea bass, Dicentrarchus labrax, for a primary lymphoid organ, the thymus, and two secondary lymphoid organs, the head-kidney and the spleen. In parallel, the oxidative burst capacity was assessed in leucocytes of the secondary lymphoid organs. Apoptosis- and proliferation-related genes, indicative of B and T cell clonal selection and lymphoid progenitor activity, were not affected by elevated oestrogen-levels. Sex-related oestrogen-responsiveness in T cell and antigen-presenting cell markers was observed, the expression of which was differentially induced by oestrogen-exposure in the three lymphoid organs. Remarkably, in the spleen, oestrogen increased regulatory T cell-related gene expression was associated with a decrease in oxidative burst capacity. To the best of our knowledge, this study indicates for the first time that physiological levels of oestrogen are likely to promote immune tolerance by modulating thymic function (i.e., T cell development and output) and peripheral T cells in teleosts, similar to previously reported oestrogenic effects in mammals. (C) 2018 Elsevier Ltd. All rights reserved.

Highlights

► 17β-oestradiol modulates peripheral and central T cell differentiation in sea bass. ► 17β-oestradiol stimulates Treg and γδ T cell differentiation and activity. ► Treg and γδ T cell stimulation was associated with immune tolerance in the spleen. ► Apoptosis and proliferation were not affected by 17β-oestradiol.

Keywords : Thymus, Spleen, Head-kidney, Teleost, Regulatory T cell, Gamma-delta T cell

Please note that this is an author-produced PDF of an article accepted for publication following peer review. The definitive publisher-authenticated version is available on the publisher Web site.

Abbreviations: AIRE, autoimmune regulator; APC, antigen-presenting cell; E2, 17β-oestradiol; EE2, 17α-ethinylestradiol; ETP, early thymic progenitor; FOXN1, forkhead-box n1; FOXP3, forkhead-box p3; H_2DCFDA, 2',7'-dichlorodihydrofluorescein diacetate; GSI, gonado-somatic index; HSI, hepato-somatic index; *K,* Fulton's condition factor; MFI, Mean Fluorescent Intensity; MHC, major histocompatibility complex; P_i, inorganic phosphorus; PCNA, proliferating cells nuclear antigen; PMA, phorbol 12-myristate 13-acetate; RAG1, recombination activating gene 1; ROS, reactive oxygen species; SSI, spleno-somatic index; TCR, T cell receptor; TEC, thymic epithelial cell; Treg, T regulatory cell; TSA, tissue specific antigen

1. Introduction

In all jawed vertebrates, T cells constitute the central component of the adaptive immunity, which develops in the thymus. The thymus represents an evolutionary innovation of the vertebrate lineage related to the appearance of somatic gene recombination and the production of a high diversity of receptors that recognize and fend off abnormal cells (Boehm and Swann, 2014; Rauta et al., 2012). Despite its early evolutionary appearance, the number of thymic glands per animal, their anatomical location, developmental origin and functional processes may differ in some detail (Bajoghli et al., 2015; Boehm and Swann, 2014; Rodewald, 2008).

The vertebrate immune system has been recognised to interact with the endocrine system (*e.g.*, Lutton and Callard, 2006; Segner et al., 2017). This crosstalk is, notably, characterized by a sexual dimorphism in immune system performance extensively described for mammals, but also occasionally reported for birds, reptiles, amphibians and teleosts (Segner et al., 2017). In mammals, oestrogens are key immunomodulatory hormones, known to modulate T cell development and function (Hince et al., 2008; Straub, 2007). Although oestrogens appear to be evolutionary ancient immunomodulators (Burgos-Aceves et al., 2016; Segner et al., 2017; Straub, 2007; Szwejser et al., 2016), knowledge about their effects on T cells in fish is scarce.

T cell-function is based on the specificity of a T cell receptor (TCR), formed by a membrane heterodimer composed either of TCRγ and δ chains or of TCRα and β chains, defining two fundamentally different T cell lineages. γδ T cells have innate-like properties and bind antigens directly while αβ T cells, or conventional T cells, recognise antigen peptides presented by the major histocompatibility complex (MHC) of type I or II (Boehm and Swann, 2014; Buonocore et al., 2012; Chien et al., 2014; Wan et al., 2017). In the thymus, αβ T cells differentiate into single positive CD8 and CD4 T cells, also referred as cytotoxic and helper T cells, respectively, by recognition of the peptide-MHC-I or II complex (Klein et al., 2014; Nakanishi et al., 2015). MHC-I is expressed by all cell types and MHC-II by specialised antigen-presenting cells (APCs), such as dendritic cells, macrophages and B cells (Esteban et al., 2015; Lewis et al., 2014; Wilson, 2017).

APCs are important for immune tolerance because they must perform several steps of αβ T cell selection, including central (positive and negative selection) as well as peripheral selection to screen clones able to discriminate self from non-self (Audiger et al., 2017; Boehm and Swann, 2014; Li and Rudensky, 2016). APCs also promote specific activation and differentiation of helper T cells or regulatory T cells (Tregs), another type of single positive CD4 T cells of great

importance for immune tolerance. In fact, Tregs regulate innate and adaptive immune cell activity and maintaine self- and non-self-tolerance (Audiger et al., 2017; Li and Rudensky, 2016; Steinman and Banchereau, 2007).

The thymus provides, maintains and restores the peripheral T cell-repertoire (Boehm and Swann, 2014; Manning and Nakanishi, 1996). The teleost thymic and peripheral T cell differentiation is depicted in figure 1, providing a conceptual framework for the choice of gene markers used in this study. The transcriptional factor Ikaros is expressed in early T cell progenitors (ETP) deriving from the head-kidney (Fig. 1.2 A; Bajoghli et al., 2009; Lam et al., 2004). ETP homing, T cell commitment and maturation is accomplished by thymic epithelial cells (TEC) under the regulation of transcription factor forkhead-box n1 (FOXN1, Bajoghli et al., 2009; Žuklys et al., 2016) and recombination-activating genes (RAG) 1 and 2 allow for the rearrangement of TCRδ, γ, β and α gene segments assuring commitment to αβ or γδ T cell subtypes (Fig. 1.2 B; Bajoghli et al., 2015; Muñoz-Ruiz et al., 2017; Yui and Rothenberg, 2014). T cell fate involves MHC-II+ cells (APCs), such as medullary thymic epithelial cells (mTEC), under the regulation of transcription factor AIRE (autoimmune regulator) (Fig. 1.2 C and 1.3; (Anderson and Su, 2016; Bajoghli et al., 2015; Saltis et al., 2008). Treg differentiation and function is regulated by forkhead-box p3 (FOXP3) transcription factor (Fig. 1.2 C and 1.3; Li and Rudensky, 2016; Quintana et al., 2010; Sugimoto et al., 2017). Immune cell homeostasis and tolerance may involve steps of apoptosis mediated by (1) the extrinsic pathway *via* Caspase-8 and (2) the intrinsic pathway *via* Caspase-9 (Audiger et al., 2017; Bouillet and O'Reilly, 2009; Daley et al., 2017; Luzio et al., 2013).

In teleosts, the head-kidney and spleen constitute the major secondary lymphoid organs (Parra et al., 2013; Rauta et al., 2012; Zwollo, 2016). The spleen is present in all jawed vertebrates, whereas the head-kidney is only found in teleost fish (Boehm and Swann, 2014; Parra et al., 2013). Because lymphopoiesis as well as T cell activation are highly dependent on proliferation (Boehm and Swann, 2014; Chien et al., 2014; Nakanishi et al., 2015), the proliferating cells nuclear antigen (PCNA) gene was also analysed in all three lymphoid organs.

To elucidate the effects of 17β-oestradiol (E2) on central and peripheral T cells, European sea bass (*Dicentrarchus labrax*) were injected with E2. The resulting changes in E2-levels, were confirmed by several known plasmatic parameters, such as Ca^{2+}, P_i or Vtg. The relative expression of *ikaros, rag1*, *foxn1* and *aire* were analysed in the thymus (Fig. 1) because they represent thymus specific function and steps of T cell development. In addition, *caspase8*,

caspase9, mhc2α chain (*mhc2a)*, *tcra*, *foxp3* and *tcrg* were analysed in the thymus, in the head-kidney and in the spleen. To corroborate the changes in activity and differentiation of T cells with innate immune cell competence, the capacity of oxidative burst was measured in leucocytes isolated from the spleen and the head-kidney.

2. Materials and Methods

2.1. Animals

A cohort of fingerlings of *D. labrax* were obtained from the hatchery "L'écloserie marine de Gravelines" (Gravelines, France) and raised in the facilities of "Aquacaux" (Octeville, France) in 1,800 L tanks with continuous flow of filtered and aerated marine seawater at environmental temperatures until about three years of age. At this time, the population comprised adolescent males and females. A few males showed signs of beginning sexual maturity, but the majority of animals were still sexually immature (see GSI in Table 1). The animals were fed daily *ad libidum* with "Turbot label rouge" fish feed (Le Gouessant, Lamballe, France). All fish were handled in accordance with the European Union regulations concerning the protection of experimental animals (Dir 2010/63/EU).

2.2. Treatment and sampling

Two successive exposure experiments were carried out, within one week of interval (Fig. S1). The fish were allotted randomly to either of the experiments and did not differ significantly with respect to the different physiological and developmental biometric indices (see supplementary data, Fig. S2), so that the data of both experiments were combined. For details on the experimental setup and validation of the experimental combination see supplementary materials and methods. Experimental conditions were the same as for hatchery (Table 1) and monitored at each injection time using a Multiparameter Meter (HI 9828, HANNA instruments, Woonsocket, USA). Fish received three consecutive intra-peritoneal injections of 0.5 mg E2/kg, prepared according to Pankhurst et al. (1986), or vehicle alone (*i.e.*, organic colza oil) at day 1, day 2 and day 6 (for details on E2-solution preparation see supplementary materials and methods). At day 7, all fish were anesthetized with tricaine methanesulfonate (MS 222; Sigma, St. Louis, USA) before weight and total length were recorded. A blood sample was taken from the caudal vein with a heparinised syringe, centrifuged at 1,000 *g* and 4 °C for 10 min, followed by a subsequent centrifugation of the supernatant at 3,000 *g* and 4 °C for another 10 min. The plasma was snap frozen and stored at -80 °C until analyses of vitellogenin- (Vtg), E2-, cortisol-

, Calcium- (Ca^{2+}), and inorganic phosphorus- (P_i) levels were carried out; sample sizes for each treatment group and measurement are specified in Table 2. The fish were sacrificed by an overdose of MS 222 and subsequent decapitation, thymus, head-kidney, spleen, liver and gonads were dissected. Individual tissue samples of thymus, head-kidney and spleen was immediately frozen in liquid nitrogen and stored at -80 °C for later RNA extraction. A part of head-kidney and spleen was gently passed through a 100 µm cell strainer adding Leibovitz medium (L15, Sigma) and kept two hours at 4°C for leucocyte isolation and flow cytometry. Gender was determined by macroscopic observation and confirmed *post hoc* by gonad histology. The total length and weight of the fish body, liver, gonads and spleen were used to establish the Fulton's condition factor (*K*), the hepato-somatic (HSI), the gonado-somatic (GSI) and the spleno-somatic (SSI) indices according to Hadidi et al. (2008), Robinson et al. (2008) and Zha et al. (2007), respectively: K (g/cm^3) = body weight (g) / total length (cm)^3 x 100 ; HSI (%) = liver weight (g) / body weight (g) x 100 ; GSI (%) = gonad weight (g) / body weight (g) x 100. Sample sizes per measurement and treatment group are specified in Table 2.

2.3. Hormone and mineral plasma levels

E2-, cortisol-, Ca^{2+}- and P_i-levels were quantified in duplicate for each fish as previously described (Pinto et al., 2016). The E2- and cortisol-levels were analysed by radioimmunoassay using specific antiserum against E2 (Guerreiro et al., 2002) and cortisol (Rotllant et al., 2005). Free hormones of the heat-denaturated plasma samples were separated using dextran-coated charcoal. Total plasma Ca^{2+}- and P_i-levels were quantified using *o*-cresolphthalein and phosphomolybdate colorimetric assays, respectively (Spinreact 1001060 and 1001150, Barcelona, Spain).

2.4. Vitellogenin plasma levels

Plasmatic Vtg-levels were determined as described by Pinto et al. (2016). Briefly, 10 µL of plasma were diluted 1/10 in Tris buffer, pH 7.8, and mixed with an equal volume of SDS PAGE sample buffer, boiled for 5 min, centrifuged at 1,700 *g* for 1 min and run on an 8% SDS-PAGE with a prestained, dual-color SDS-PAGE molecular weight marker (ref. 161-0374, Bio-Rad Laboratories, Hercules, USA). Gels were stained with Coomassie blue, scanned and digital images captured using Alpha Imager System (Alpha Innotech, San Leandro, USA). Vtg at 180 kDa was quantified using Image J (v.1.48). Total plasma protein was determined after dilution (1:75) using the Bradford method (Bradford, 1976) with bovine serum albumin (Sigma) as a

standard. The relative plasma level of Vtg was expressed as band density (pixels/mm^2/µg total protein) of the respective sample.

2.5. Gene expression

Relative gene expression of *ikaros, rag1, foxn1 and aire* was assessed in the thymus only. Gene expression of *tcra, foxp3, tcrg, pcna, mhc2a, caspase8, caspase9,* the elongation factor α 1 (*ef1a*), the ribosomal protein L13 a gene (*l13a*) and the 40S ribosomal protein S30 (*fau;* for sequence determination procedure see supplementary materials and methods) was assessed in the thymus, the head-kidney and the spleen. For sample sizes per treatment group and analysis the reader is referred to Table 2. Details on the respective primers are given in Table S3. Total RNA was extracted using Tri Reagent® (Sigma) according to the supplier's instructions. Tissue samples were homogenised twice in Precellys® tubes (CK14; Bertin instruments, Montigny-le-Bretonneux, France) for 10 s at 5,000 rpm and subsequently centrifuged at 12,000 *g* for 15 min at 4 °C to eliminate debris. After RNA extraction, possible DNA contamination was removed by digestion with the TURBO DNA-*free* Kit (Invitrogen-Ambion, Carlsbad, USA) according to the supplier's instructions. RNA quality was assessed on 1 % agarose gels and the yield was quantified with a Nanodrop One (ThermoFisher, Waltham, USA) at 260 nm and 280 nm. Absorbance ratios 260/280 between 1.93 and 2.01 indicated pure RNA samples. Samples were stored at -80 °C until further processing.

Reverse transcription was performed using 1 µg of RNA, 0.5 µg of Oligo(dT), dNTP and M-MLV RT (Promega, Fitchburg, USA) with an incubation of 5 min at 70 °C and 60 min at 42 °C at a final volume of 25 µL and cDNA was stored at -20 °C. Real-time qPCR was performed using three technical replicates per individual sample (*i.e.*, biological replicate corresponding to the n given in table 2) by separately adding cDNA diluted 1:20 in DNase/RNase free water. Different reaction volumes were employed according to the respective gene and thermocycler combination used for qPCR (Table S3). Two genes (*tcrg* and *ikaros*) were analysed in 10 µL using the Rotor-Gene Q instrument (Qiagen, Hilden, Germany) with QuantiTect SYBR® Green PCR Kit 5 (Qiagen). The twelve remaining genes were analysed in either 5 µL, or 1.5 µL with the LightCycler® 480 Instrument II (Roche Molecular Diagnostics, Pleasanton, USA) with LightCycler® 480 SYBR Green I Master (Roche). Different reaction volumes were used in order to adjust the cycle threshold between different genes. A plate linker sample was run on all plates for each given gene. For the final volume of 1.5 µL reaction mix, 0.5 µL of cDNA and 1 µL of PCR mix (enzyme, dNTP and primers) were loaded on a 384-microwell plate using

a Labcyte Acoustic Automated Liquid Handler (Echo® 525, Labcyte™, San Jose, USA; GenomiX platform, Montpellier University). The use of the Labcyte Echo enables miniaturization of qRT-PCR assay (Agrawal et al., 2016; Green et al., 2016). Oligonucleotides were used at a final concentration of either 0.5 µM or 0.75 µM as optimized for each gene (Table S3). Negative controls were performed with DNA free water. For LightCycler® 480 SYBR Green I Master qPCR conditions were as follows: initial incubation at 95 °C for 10 min followed by 45 cycles at 95 °C for 10 s, 60 °C for 10 s (for primer specific hybridization temperature see Table S3) and 72 °C for 10 s. The QuantiTect qPCR conditions were: 95°C for 15 min, 94 °C for 15 s, 60 °C for 30 s and 72 °C for 30 s, with the three last steps being repeated for 40 times. PCR-products were evaluated on 2% agarose gels and assessed with the qPCR melting curves. Cycle thresholds were determined either with LightCycler 1.5 480 or with Rotor-Gene Q software version 2.0.2 (Build 4). For each organ and primer pair, the PCR amplification efficiency was calculated by serial dilutions of cDNA pooled with samples of all conditions (experiment, treated, control and gender; see Table S3).

For the quantification of relative gene expression, the reference genes: *ef1a*, *l13a* and *fau* (Table S3) emerged to be stably expressed between control and treatments in males and females for each organ and experiment (Supplementary data, figure S3). The primers for *fau* and *ef1a* were previously utilized as reference genes in sea bass by Mitter et al. (2009). Furthermore, *l13a* and *ef1a* were validated as suitable references genes with xenoestrogen exposure in teleost fish (Lorin-Nebel et al., 2014; McCurley and Callard, 2008). The relative expression ratio of a target gene was calculated based on the formula of Pfaffl (2001) using the efficiency of each primer pair calculated in each organ (Table S3) and the geometric mean of the three reference genes as recommended by Vandesompele et al. (2002). Henceforth, the normalized expression of each analysed gene is referred to as 'gene expression'. Furthermore, as a control, normalization with each reference genes (*ef1a, l13a, fau*) was checked independently.

2.6. Leucocyte isolation and, assessment of the viability and population distribution

The cell solutions from head-kidney and spleen (see 2.2, "sampling") were loaded on Histopaque®-1077 (Sigma) and leucocytes were separated by centrifugation for 30 min at 400 *g* and 4 °C. The Leucocytes were collected at the interface and washed twice at 1,200 *g* and 4 °C for 5 min. The cell concentration was determined with a hemocytometer and adjusted to $1x10^6$ cells per mL. Cell mortality was assessed as described by Seemann et al. (2016). Briefly, the cells were incubated with 50 µg/mL of iodide propidium at room temperature for 10 min in

obscurity. The different cells types were defined by their granularity/internal complexity (SSC, side scatter) and their electronic volume. In agreement with previous work (Granja et al., 2015; Seemann et al., 2016), two populations were identified: the lymphoid and myeloid cells, the former being of larger size and granularity. The mortality was assessed as the percentage of lymphoid and myeloid cells with high red fluorescence. The population distribution corresponded to the percentage of events in either of the gates for each cell type. Each flow cytometric measurement was conducted with 25,000 events in the gate "cells" comprising both cell types. The analyses of flow cytometry were conducted using the Cell Lab Quanta SC MPL flow cytometer (Beckman Coulter) and the software FlowJo® (version 8.7, Ashland, Oregon, USA).

2.7. Respiratory burst

Respiratory burst was assessed on leucocytes isolated from the head-kidney and spleen as described by Bado-Nilles et al. (2014) (The analysed sample sizes in each treatment group are specified in Table 2). Briefly, for each sample two aliquots of cells were incubated with 5 µM of 2',7'-dichlorodihydrofluorescein diacetate (H_2DCFDA, ThermoFisher) for 30 min. Subsequently, one aliquot was stimulated for 30 min using 2 µg/mL of phorbol 12-myristate 13-acetate (PMA, Sigma). The membrane permeant H_2DCFDA is converted by intracellular oxidases and esterases to a non-fluorescent product, which reacts with reactive oxygen species (ROS) and converts it to the highly fluorescent 2',7'-dichlorofluorescein (DCF). The green fluorescence of the unstimulated and stimulated cells was measured for each gate (lymphoid and myeloid cells) with 25,000 events in the gate "cells". Three different measurements were carried out: the stimulation index of respiratory burst as the ratio of the mean fluorescent intensity (MFI) of stimulated cells to unstimulated cells and the MFI (expressing the level of ROS) of the stimulated and unstimulated cells.

2.8. Statistical analysis

All statistical analyses were conducted using SigmaPlot (version 12.0, Systat Software Inc., San Jose, USA), unless otherwise stated. Gene expression data are reported as normalised expression and visualized as box-and-whisker plots, indicating the median, the 25 and 75 percentiles as well as the minimum and maximum values. The results of flow cytometry are depicted as histograms with means and standard errors (S.E.). Prior to analyses, outliers were eliminated using the Grubb's outlier test (for combined data from all groups, ©2017 GraphPad Software Inc., La Jolla, USA). The datasets were checked for normality and equal variances

using the Shapiro-Wilk test and the Levene Median test, respectively. Subsequently, pairwise analysis was conducted to compare E2- and CTR-groups for both genders separately. Were significant differences between treatments absent, E2- and CTR-groups were combined to check for possible gender differences. If normal distribution and homoscedasticity could be confirmed, an independent Student *t*-test was used for pairwise parametric hypothesis testing; otherwise non-parametric Mann-Whitney *U*-test was conducted. Pairwise linear correlations were assessed for each grouped data (CTR-F, E2-F, CTR-M and E2-M with experiments combined) for plasmatic E2, cortisol and gene-expression levels using the non-parametric Spearman rank order correlation. The *p*-values were adjusted for multiple hypotheses testing by the False Discovery Rate procedure (Benjamini and Hochberg, 1995), which was set to 15 %. The results were considered significant at an α-level of 0.4% ($p<0.004$) as determined by the False Discovery Rate.

3. Results

3.2. Exposure validation

The efficacy of the E2-treatment was validated by the changes in the plasmatic levels of E2, Ca^{2+} and P_i as well as by the changes in the HSI for CTR-M, CTR-F, E2-M and E2-F from both experiments combined (the exact sample sizes of which are displayed in Table 2). When comparing males and females from the CTR- and E2-groups (Fig. 2, Table 1), a significant difference in the plasmatic E2-level (*Kruskal-Wallis*, $H_{3,60}=49.54$, $p<0.001$) was revealed. Also, the HSI values (*Kruskal-Wallis*, $H_{3,61}=36.75$, $p<0.001$), Ca^{2+} (*Kruskal-Wallis*, $H_{3,61}=37.58$, $p<0.001$) and P_i (*Kruskal-Wallis*, $H_{3,68}=15.38$, $p=0.001$) were significantly different. The Tukey-Kramer *post-hoc* analyses demonstrated that the E2-exposure significantly increased plasmatic concentrations of E2 from 0.040 ng/mL ± 0.023 s.d. to 2.640 ng/mL ± 1.943 s.d. in females and from 0.044 ng/mL ± 0.029 s.d. to 3.560 ng/mL ± 0.432 s.d. in males (both $p<0.001$; all *p*-values are listed in Table S10). The Tukey-Kramer *post-hoc* analyses indicated a significant increase for the HSI following E2-treatment in females and males (both $p<0.001$; all *p*-values are listed in Table S11). The Ca^{2+}- and the P_i-levels of the E2-exposed animals were significantly increased in females only (both $p<0.001$, Tables S12 and S13).

Comparing the CTR and the E2-treatments for males and females combined (Fig. 2, Table 1), the E2-exposure significantly increased the plasmatic concentrations of E2 (*U*-test, $p<0.001$).

A significant increase of Ca^{2+} (*U*-test, $p<0.001$) and a significant increase of P_i from (*U*-test, $p<0.001$) as well as a significant increase of Vtg (*U*-test, $p=0.018$) could also be observed.

3.2. Gene expression

Relative gene expression was compared for CTR-M, CTR-F, E2-M and E2-F from both experiments combined with sample sizes ranging from n=5 to 15 (exact sample sizes per group and organ are provided in Table 2).

3.2.1. Thymic homing, T cell maturation and TEC function

E2-treatment did not modulate *ikaros* expression in females (*t*-test, $p=0.848$; Fig. 3), which, however, tended to increase in males (*t*-test, $p=0.393$). The E2-treatment decreased the *rag1*-expression level in E2-F, but this was not statistically significant (*U*-test, $p=0.238$; Fig. 3). No significant change of *rag1* expression level could be detected in E2-M (*t*-test, $p=0.770$).

The E2-treatment did neither significantly decrease *foxn1* expression (Fig. 3) in females (*U*-test, $p=0.696$), nor in males (*t*-test, $p=0.963$). However, the E2-treatment affected the significantly positive correlation of *foxn1* with *ikaros* and *foxp3* (Table 3 and Table S14), which was observed in CTR but not in E2-treated females.

3.2.2. Thymic and peripheral T cell selection

The E2-treatment significantly increased *aire*-expression levels (Fig. 3) in females (*U*-test, $p=0.007$), but not in males (*t*-test, $p=0.822$).

E2-treatment significantly increased *mhc2a* expression in the thymus of males, but not in females (*t*-test, $p=0.038$ and p=0.386, respectively; Fig. 4). This was, however, not the case in the head-kidney of E2-exposed males (Fig. 4), where a trend to increased *mhc2a*-expression level in females was observed (*t*-test, $p=0.253$ and *t*-test, $p=0.096$, respectively). In the spleen, E2-treatment did neither affect *mhc2a* expression in males, nor in females (*t*-test, $p=0.476$ and *t*-test, $p=0.890$; Fig. 4).

E2-treatment did not significantly modulate the expression-levels of *caspase8* and *caspase9* (Fig. 4), neither in the thymus of females (*U*-test, $p=0.800$ and $p=0.781$, respectively), nor that of males (*t*-test, $p=0.923$ and $p=0.141$, respectively). The same was observed in the head-kidney of females (*t*-test, $p=0.947$ and $p=0.856$, respectively) and males (*t*-test, $p=0.136$ and *U*-test, $p=0.704$) as well as in the spleen of females (*t*-test, $p=0.999$ and $p=0.341$, respectively) and males (*U*-test, $p=0.661$ and $p=0.950$, respectively).

The correlations between *caspase9* and *caspase8* with *ikaros, foxn1*, as well as *pcna* in the thymus of female are presented in Table 3 and Table S14. In CTR-F, the expression-level of *caspase9* was significantly correlated with *ikaros* and *foxn1.* Also in CTR-F, *capsase8* expression was significantly correlated with *pcna.* Similar correlations were not observed in E2-F.

Correlations between the expression-level of *caspase9* and *caspase8* with *foxp3, tcra* and *tcrg* as well as *mhc2a* in the head-kidney and spleen are presented in Tables 3 and 4 as well as Table S15-18. In the head-kidney, *caspase9* expression showed a significantly positive correlation with *foxp3* in both CTR-F, but not in E2-F (Table 3 and Table S15), whereas this positive correlation was not altered in E2-M, as compared to CTR-M (Table 4 and Table S16).

3.2.3. Cell proliferation

Following E2-treatment, *pcna* expression (Fig. 4) appeared to decrease in females, but this decrease was not statistically significant for any of the three lymphoid organs (*U*-tests for thymus, head-kidney, spleen: p=0.200, p=0.366, p=0.079; respectively), whereas no effect occurred in E2-M (*t*-tests for thymus and head-kidney, p=0.981, p=0.351, respectively; *U*-test for spleen, p=0.885).

The *pcna* expression in the head-kidney was positively and significantly correlated (Table 3 and Table S15) with *mhc2a* in CTR-F. This positive correlation was lost in E2-F.

3.2.4. T Cell subtypes

In the thymus, E2-treatment tended to decrease the expression-level of *tcra* (Fig. 5) in E2-F (*t*-test, p=0.154), whereas it did not affect E2-M (*t*-test, p=0.286).

In the head-kidney, E2-treatment increased the expression-level of *tcra* (Fig. 5) in females, but did not modulate the *tcra* expression in males (*t*-test, p=0.023 and p=0.430, respectively). In the head-kidney of CTR-F and E2-F, *tcra* and *pcna* expression showed no significantly positive correlation (Table 3 and Table S15). In the head-kidney, E2-M showed a significantly positive correlation between *tcra* and *mhc2a* (Table 4 and Table S16); a similar correlation was not observed in CTR-M.

In the spleen, E2-treatment did not increase the expression-level of *tcra* in females (*t*-test, p=0.605), but it tended to increase in males, albeit not significantly (*U*-test, p=0.083).

In the E2-treated fish (Fig. 5), the expression level of *foxp3* increased significantly in the thymus of E2-M (*t*-test, p=0.036), but did not in E2-F (p=0.258, *t*-test).

In the head-kidney, *foxp3*-expression level was neither modulated in males, nor in females (*t*-test, p=0.642 and p=0.268, respectively; Fig. 5). In the spleen, the expression-level of *foxp3* was increased in females, but not in males (*t*-test, p=0.021 and p=0.860, respectively). In the male spleen, the E2-treatment resulted in a significantly positive correlation of *foxp3* with *mhc2a* and *pcna* (Table 4 and Table S18). Similar correlations were not observed in the spleen and head-kidney of CTR-F, CTR-M and E2-F (Table 3-4 and Table S15-18).

The E2-treatment did neither modify the expression-level of *tcrg* in the thymus of E2-F (*U*-test, p=0.452; Fig. 5), nor in E2-M (*t*-test, p=0.998). However, female thymuses generally, had a lower *tcrg* expression than those of males (*U*-test CTR-F+E2-F *vs.* CTR-M+E2-M combined, p=0.020). In head-kidney and spleen, the E2-treatment increased the expression-level of *tcrg* in E2-M (*t*-test, p=0.037 and p=0.030, respectively), but had no effect in E2-F (*U*-test, p=0.869, *t*-test, p=0.170). In spleen, the E2-M showed a positive and strong correlation (Table 4B and Table S18) between *tcrg, mhc2a* and *pcna*. Similar correlations were not observed in the spleen of CTR-M, CTR-F and E2-F, nor in the head-kidney of E2-M, CTR-M and E2-F (Table 3-4A and Table S15-18).

In CTR-M, but not E2-M, the expression of *tcrg* in the head-kidney and spleen were positively and significantly correlated (r=0.850 p<0.001; r=0.393, p=0.341).

3.3. Flow cytometry

Respiratory burst was assessed by flow cytometry for CTR-M, CTR-F, E2-M and E2-F from both experiments combined with sample sizes ranging from n=4 to 10 (exact sample sizes per group and organ are displayed in Table 2)

3.3.1. Leucocytes mortality and distribution

E2-treatment did neither significantly alter the mortality of the lymphocytes and myeloid cells isolated from the head-kidney (*t*-test, p=0.126 and p=0.961, respectively), nor from the spleen (*t*-test, p=0.601 and p=0.485, respectively) (Fig. 6b). In addition, no effect of E2-treatment was observed for the population distribution of isolated leucocytes from the head-kidney and spleen.

3.3.2. Oxidative Burst

E2-treatment did not affect the basal ROS-level (unstimulated, *i.e.*, without PMA) of isolated leucocytes from the head-kidney or the spleen (Fig. 6c). Similarly, no statistically significant effect of E2-treatment on the ROS-levels of stimulated (*i.e.*, with PMA) lymphocytes and

myeloid cells isolated from the head-kidney could be observed (*t*-test, p=0.914; *U*-test, p=0.361 respectively). On the contrary, E2-treatment significantly decreased the ROS-levels of stimulated cells (with PMA) from the spleen: the MFI in lymphocytes of E2-treated animals was less than half as compared to controls (44.03 ± 11.41 s.e. *vs*. 94.38 ± 14.98 s.e.; *U*-test, p=0.016) and about the same was observed in myeloid cells (223.6 ± 54.77 s.e. *vs*. 446.9 ± 17.85 s.e.; *U*-test, p=0.016). The oxidative burst index for lymphocytes of the head-kidney remained unaffected by E2-treatment (CTR 3.89 ± 0.46 s.e. *vs*. E2 3.90 ± 0.40; *U*-test, p=0.836), as was the case for myeloid cells (CTR 6.315 ± 0.736 s.e. *vs*. E2 7.824 ± 1.039; *U*-test, p=0.333). In the spleen, E2-treatment significantly decreased the oxidative burst index in lymphocytes with 3.205 ± 0.424 s.e. in CTR *vs*. 1.854 ± 0.420 in E2-treated fish (*U*-test, p=0.022). A similar effect seemed to occur in the myeloid cells from the spleen with 4.770 ± 0.467 in CTR *vs*. 3.488 ± 0.756 in E2-treated animals, but without this difference being statistically significant (*t*-test, p=0.168).

4. Discussion

The three intra-peritoneal injections with E2 over one week lead to clearly elevated E2-plasma levels, which were similar to concentrations observed in female sea bass during the spawning season (Mañanós et al., 1997; Navas et al., 1998). Hence, the E2-treatment was both efficient and situated within the physiological range of E2-titers. The effectiveness of the E2-treatment, was further underscored by a significant increase of Ca^{2+}-, P_i- and Vtg-levels in the serum, all of which are known to be induced by E2 (Nelson and Habibi, 2013; Pinto et al., 2016). As the liver produces Vtg, the increased HSI is coherent with an E2-stimulated Vtg-synthesis. Similarly, an increase of the HSI has been observed after 17α-ethynylestradiol (EE2) treatment in other teleost species (Rodenas et al., 2016; Zha et al., 2007).

According to the oestrogenic modulation of the adaptive immune system and the thymus plasticity described for teleosts and other vertebrates (Lutton and Callard, 2006; Seemann et al., 2015; Segner et al., 2017; Szwejser et al., 2016), this study suggests that E2 modulates thymic and peripheral T cell maturation in a complex manner, as outlined in the following.

4.1. Thymic T cell development and release

4.1.1. Thymic homing

The ETPs are represented by *ikaros* expression, which, in zebrafish, is up-regulated before ETPs begin to express *rag1*. This probably occurs after progenitor cells are committed to the T

cell lineage, just like in mammals (Fig. 1.2 A; Lam et al., 2004; Yui and Rothenberg, 2014). E2-treatment of sea bass did not significantly affect the expression-level of *ikaros* in our experiments. This suggests that the colonization of the thymus by ETPs was not modulated by physiological E2-levels, as opposed to the rapid decline of ETPs observed in mice after E2-injection or during pregnancy (Zoller et al., 2007; Zoller and Kersh, 2006).

4.1.2. T cell maturation and TEC function

The T cell maturation, selection and differentiation involves the transcription factors FOXN1 and AIRE expressed in TEC (Fig. 1.2; Abramson and Anderson, 2017; Anderson and Su, 2016; Bajoghli et al., 2015, 2009; Saltis et al., 2008; Žuklys et al., 2016). In the thymus of sea bass, E2-treatment did not significantly affect the expression-level of *foxn1*. However, the E2-treatment (1) increased the *aire*-expression level, and (2) eliminated the significant correlation of *foxn1*-expression levels with *ikaros* and *foxp3* in females, which suggests that E2 modulated TEC function and thereby thymic T cell maturation (Bajoghli et al., 2015; Klein et al., 2014). These observations are in good agreement with the mammalian oestrogenic modulation of TEC function demonstrated both *in vivo* and *in vitro* (Dragin et al., 2016; Jin et al., 2003; Martín et al., 1995a).

4.1.3. T cell lineage subtype commitment

Early RAG1/2+ T cell lineage committed progenitors possibly differentiate into γδ or αβ T cells (Fig. 1.2 B). In sea bass, E2 tended to decrease the expression of *rag1* in the thymus of females. This suggests that E2 does not halt early T cell maturation in teleosts, as proposed for mammals (Bernardi et al., 2015; Rijhsinghani et al., 1996). The γδ selection is characterized by the expression of TCRγδ and, to some extent, by a lower proliferation in comparison to the β-selected cells (Muñoz-Ruiz et al., 2017; Turchinovich and Pennington, 2011; Yui and Rothenberg, 2014). In the present study, expression of *tcrg* in the thymus was not affected by E2-treatment, neither in males, nor females. Female sea bass, however, expressed significantly lower levels of *tcrg.* In addition, E2 tended to decrease the relative expression of *pcna* in female sea bass. Overall, these results suggest that sex steroids, such as E2, have the potential to modulate T cell subtype commitment. Because E2-treatment did not change the expression-level of *tcra* in the thymus of males and females, there was no indication of E2 affecting the αβ T cell lineage. This suggests that the main thymic T cell lineage, *i.e.*, the αβ T cell, would remain weakly affected after one week of elevated physiological E2-levels.

In the mammalian thymus, E2-exposure increased the proportion of T cells with mature phenotypes CD3, CD4 or CD8 SP. Therefore, E2 was presumed to stimulate an alternative intrathymic pathway of CD4 and CD8 double negative T cell maturation including αβ and γδ T cells (Abo, 2001; Chapman et al., 2015; Rijhsinghani et al., 1996; Screpanti et al., 1991). Except for the γδ T cells, this intrathymic pathway could not be directly evidenced for the sea bass thymus, because, although sex-depended differences existed, no treatment effect became visible. Any confirmation of whether such an alternative intrathymic pathways exists, or not, is, however, hampered by the lack of specific markers, which can distinguish between the unconventional T cells (Cheroutre et al., 2011).

4.1.4. Central tolerance

The increase of *aire* and *mhc2a* expression in male and female sea bass following E2-treatment could indicate an increased central tolerance (Fig. 1.2 C). Interestingly, *aire* expression in mammals is also regulated by oestrogen, where it was, however, reported to decrease the number of AIRE+ TECs and AIRE expression in TECs, resulting in a decrease of AIRE-dependent tissue specific antigens-production and an increase in the prevalence of autoimmune diseases (Anderson and Su, 2016; Dragin et al., 2016; Klein et al., 2014). Given the potential functional conservation of AIRE and MHC-II in T cell-selection of jawed vertebrates (Bajoghli et al., 2015; Lewis et al., 2014; Saltis et al., 2008), our results suggest that E2 enhanced central tolerance in female and in male sea bass.

The putative increase of central tolerance may result in increased immature T cell-apoptosis in the thymus, as it has been reported for mice or lizard (Do et al., 2002; Hareramadas and Rai, 2006; Wang et al., 2008). In sea bass, however, the E2-treatment did not affect the caspases expression. On the one hand, this suggests that in teleosts, E2 does not strongly affect T cell-apoptosis. On the other hand, the lack of an obvious E2-induced apoptosis is in agreement with the observations of Chapman et al. (2015), who proposed that E2 does not enhance thymic T cell-apoptosis at physiological concentrations.

The increase of central tolerance may also result in an increase of Treg differentiation. For instance, the proportion of thymus-derived Treg increased with elevated E2-levels observed in early pregnancy of mice (Teles et al., 2013). Interestingly, in male sea bass, the expression of *foxp3* increased concomitantly to the increase in *mhc2a* expression, suggesting that E2 induced Treg differentiation. This observation provides additional support for the E2-induced central tolerance in sea bass.

4.1.5. T cell migration

Considering the peripheral αβ T cells (Fig. 1.3), we observed that E2-treatment significantly increased the expression-level of *tcra* in the head-kidney of females. It also tended to increase *tcra* in the spleen of males. These changes could derive from T cell-activation, characterized by a stimulation of proliferation. As no significant increase of *pcna* expression was observed and no correlation between the expression-levels of *pcna* and *tcra* could be determined, one may hypothesise that the increase of *tcra* expression is due to an increased αβ T cell input in the head-kidney. These αβ T cells are probably coming from the thymus, which is the main source of T cells (Boehm and Swann, 2014; Manning and Nakanishi, 1996). This interpretation is in line with the rapid increase of the number of T cells in the head-kidney of gilthead sea bream following EE2-exposure observed by (Rodenas et al., 2017). Likewise, these authors could not detect any effect of E2 on T cell proliferation.

As for the peripheral γδ T cells, E2-treatment resulted in an (1) increase of *tcrg* expression in the head-kidney and the spleen of male sea bass, and a (2) strongly positive correlation of *tcrg* with *pcna* and *mhc2a* in spleen, but not in the head-kidney. Because mammalian γδ T cells can show clonal expansion (Chien et al., 2014), and because γδ T cells express MHC-II (Chien et al., 2014; Wan et al., 2017), our observations suggest that E2 induced proliferation and entry of γδ T cells in the spleen and the head-kidney, respectively. Furthermore, it may be assumed that γδ T cells of the head-kidney and spleen represent two distinct populations.

These interpretations, together with the lower expression of *tcrg* in the thymus of females as well as the potentially E2-induced increase of αβ T cells in the head-kidney of females, suggest that E2 induced thymic T cell output in sea bass, similar to observations made in mammals (Chapman et al., 2015; Martín et al., 1995a). This T cell-release is believed to be promoted by a E2-mediated vasodilatation, which is induced by thymic mast cell-activation (Chapman et al., 2015). A similar mechanism may be assumed in sea bass, as Paiola et al. (2017) detected nuclear and membrane oestrogen receptor expression in the thymic vessels and mast cells of *D. labrax*. In mammals, these E2-mediated changes of T cell output have been associated with a stimulation of an alternative intrathymic pathway of T cell maturation (Abo, 2001; Chapman et al., 2015). Similar effects are, therefore, likely to occur in the thymus of sea bass.

4.1.6. Thymic APC migration and differentiation

Because E2 increased *mhc2a* expression in the thymus of males, one may assume that E2 stimulated antigen presentation in the thymus of male sea bass, as it was described for mammals (Wira et al., 2003). Correspondingly, in the mammalian thymus, E2 increases thymic migration and/or differentiation of several potential APCs, such as B cells, plasma cells, macrophages and

granulocytes (Martín et al., 1994, 1995b; Ross and Korenchevsky, 1941). The increase of *foxp3* in males, which occurred concomitantly to the increase of *mhc2a* expression, corroborates this interpretation. As a matter of fact, an increased number of APCs (both mTEC and DC) has been shown to stimulate thymus-derived Treg generation (Abramson and Anderson, 2017; Lin et al., 2016). This would confirm that E2 modulates T cell fate in the thymus of sea bass.

4.2. Peripheral tolerance and T cell differentiation

In the periphery, naïve and mature T cells undergo supplementary selection and differentiation (Fig. 1.3). At first sight, E2 did not alter B and T cell clonal selection, because caspase gene expression was not significantly modulated by E2-treatment. This interpretation is further underscored by an unaltered leucocyte viability in the spleen and head-kidney following E2-treatment. At closer examination, however, E2-treatment strongly increased the *foxp3*-expression level in the spleen of females, suggesting an E2-related induction of peripheral T cell-differentiation or migration of thymus-derived Tregs. Interestingly, a highly significant and positive correlation of *foxp3* with *mhc2a* as well as *pcna* was observed in the spleen of males following E2-treatment. By presenting peptide-MHC-II complex, APCs induce Treg differentiation followed by high level of proliferation (Li and Rudensky, 2016). Accordingly, one may assume that in the spleen of sea bass, E2 induced Treg differentiation in females and, to a lesser extent, in males. Interestingly, pregnancy as well as *in vitro* and *in vivo* E2-treatments both increased the proportion of Treg and *foxp3* expression/FOXP3-levels in the spleen of female mice (Polanczyk et al., 2004, 2005; Tai et al., 2008). This is likely to enhance the suppressive activity of Tregs (Polanczyk et al., 2005). In teleosts, FOXP3 is believed to have a similar function in Tregs (Quintana et al., 2010; Sugimoto et al., 2017; Wen et al., 2011). Therefore, the E2-mediated increase of *foxp3*-level in the spleen suggests that E2 promotes tolerance and anti-inflammatory activity through an expansion of FOXP3+ αβ Treg cells in the spleen of sea bass, similar to the situation described for mammals. This interpretation is further corroborated by the fact that the inhibition of oxidative burst capacity occurred solely in the spleen, but not in the head-kidney.

Furthermore, in the male spleen, the apparent E2-mediated anti-inflammatory response could also result from the increase of γδ T cells with a regulatory phenotype. Indeed, high E2-levels promote immune tolerance during pregnancy in mammals, by increasing peripheral γδ Tregs (Chapman et al., 2015). One may speculate that this also the case in fish, although the corresponding γδ T cell subtypes have not yet been identified in teleosts.

5. Conclusion

The results of this study covering T cell-related gene expression in the sea bass provide evidence for E2-induced immune tolerance by qualitatively and quantitatively modulating the peripheral T cell subsets in *D. labrax*. Two mechanisms are likely to be involved: (1) a modulation of the thymic function, such as the T cell lineage commitment and the release, *i.e.,* a stimulation of an intrathymic alternative pathway of T cell maturation, and (2) a modulation of the differentiation and/or the activity of mature/peripheral T cells. Similar mechanisms of E2-action on the thymus and peripheral lymphoid organs have been identified in mammals (Abo, 2001; Chapman et al., 2015; Polanczyk et al., 2005). The gender-specific behaviour of the different T cell subsets in the various lymphoid organs underscores the implication of oestrogens in these processes.

During mammalian pregnancy, the expansion of Treg, double negative αβ and γδ T cells in peripheral organs, including the spleen, is believed to be important to avoid a detrimental immune response against the semiallogenic foetus (Chapman et al., 2015; Clark, 2016). Our study suggests that the E2-induced increase in T cell-mediated peripheral tolerance is evolutionarily conserved in jawed vertebrates. In sea bass, higher plasmatic levels of E2 are associated to seasonal events including reproduction, migration as well a switch to nocturnal feeding and locomotor behaviour (del Pozo et al., 2014; Mañanós et al., 1997). Consequently, immunomodulation could be related to changes in diet, energy budget and reserves and/or environmental pathogens.

Acknowledgements: This research was supported by the ANR financed project ETaT (ANR-15-CE32-0014). M.P. was supported by the Normandy region through the FR CNRS 3730 SCALE. P.I.S.P. was supported through the Foundation for Science and Technology of Portugal (FCT), through the projects PTDC/AAG-GLO/4003/2012 and CCMAR/Multi/04326/2013 and the fellowship SFRH/BPD/84033/2012. The authors thank Matthieu Bonnet and the staff at Aquacaux for fish hatchery, Elsa Couto and Soraia Santos (CCMAR) for carrying out sea bass plasma analyses and Sandrine Crochmore for her technical support in gene expression measurements. We would like to thank Salima Aroua, Sabrina Jolly, Stéphanie Olivier, Agnès Poret and Béatrice Rocher for their assistance throughout the exposures and samplings.

Compliance with ethical standards

All applicable national guidelines for the care and use of animals were followed.

Conflict of interest: The authors declare that they have no conflict of interest.

References

Abo, T., 2001. Extrathymic pathways of T-cell differentiation and immunomodulation. Int. Immunopharmacol. 1, 1261–1273. https://doi.org/10.1016/S1567-5769(01)00057-1

Abramson, J., Anderson, G., 2017. Thymic Epithelial Cells. Annu. Rev. Immunol. 35, 85–118. https://doi.org/10.1146/annurev-immunol-051116-052320

Agrawal, S., Cifelli, S., Johnstone, R., Pechter, D., Barbey, D.A., Lin, K., Allison, T., Agrawal, S., Rivera-Gines, A., Milligan, J.A., Schneeweis, J., Houle, K., Struck, A.J., Visconti, R., Sills, M., Wildey, M.J., 2016. Utilizing Low-Volume Aqueous Acoustic Transfer with the Echo 525 to Enable Miniaturization of qRT-PCR Assay. J. Lab. Autom. 21, 57–63. https://doi.org/10.1177/2211068215609315

Anderson, M.S., Su, M.A., 2016. AIRE expands: new roles in immune tolerance and beyond. Nat. Rev. Immunol. 16, 247–258. https://doi.org/10.1038/nri.2016.9

Audiger, C., Rahman, M.J., Yun, T.J., Tarbell, K.V., Lesage, S., 2017. The Importance of Dendritic Cells in Maintaining Immune Tolerance. J. Immunol. 198, 2223–2231. https://doi.org/10.4049/jimmunol.1601629

Bado-Nilles, A., Techer, R., Porcher, J.M., Geffard, A., Gagnaire, B., Betoulle, S., Sanchez, W., 2014. Detection of immunotoxic effects of estrogenic and androgenic endocrine disrupting compounds using splenic immune cells of the female three-spined stickleback, *Gasterosteus aculeatus* (L.). Environ. Toxicol. Pharmacol. 38, 672–683. https://doi.org/10.1016/j.etap.2014.08.002

Bajoghli, B., Aghaallaei, N., Hess, I., Rode, I., Netuschil, N., Tay, B.-H., Venkatesh, B., Yu, J.-K., Kaltenbach, S.L., Holland, N.D., Diekhoff, D., Happe, C., Schorpp, M., Boehm, T., 2009. Evolution of Genetic Networks Underlying the Emergence of Thymopoiesis in Vertebrates. Cell 138, 186–197. https://doi.org/10.1016/j.cell.2009.04.017

Bajoghli, B., Kuri, P., Inoue, D., Aghaallaei, N., Hanelt, M., Thumberger, T., Rauzi, M., Wittbrodt, J., Leptin, M., 2015. Noninvasive In Toto Imaging of the Thymus Reveals Heterogeneous Migratory Behavior of Developing T Cells. J. Immunol. 195, 2177–2186. https://doi.org/10.4049/jimmunol.1500361

Benjamini, Y., Hochberg, Y., 1995. Controlling the False Discovery Rate: A Practical and Powerful Approach to Multiple Testing. J. R. Stat. Soc. Ser. B Methodol. 57, 289–300.

Bernardi, A.I., Andersson, A., Stubelius, A., Grahnemo, L., Carlsten, H., Islander, U., 2015. Selective estrogen receptor modulators in T cell development and T cell dependent inflammation. Immunobiology 220, 1122–1128. https://doi.org/10.1016/j.imbio.2015.05.009

Boehm, T., Swann, J.B., 2014. Origin and Evolution of Adaptive Immunity. Annu. Rev. Anim. Biosci. 2, 259–283. https://doi.org/10.1146/annurev-animal-022513-114201

Bouillet, P., O'Reilly, L.A., 2009. CD95, BIM and T cell homeostasis. Nat. Rev. Immunol. 9, 514–519. https://doi.org/10.1038/nri2570

Bradford, M.M., 1976. A rapid and sensitive method for the quantitation of microgram quantities of protein utilizing the principle of protein-dye binding. Anal. Biochem. 72, 248–254. https://doi.org/10.1016/0003-2697(76)90527-3

Buonocore, F., Castro, R., Randelli, E., Lefranc, M.-P., Six, A., Kuhl, H., Reinhardt, R., Facchiano, A., Boudinot, P., Scapigliati, G., 2012. Diversity, Molecular Characterization and Expression of T Cell Receptor γ in a Teleost Fish, the Sea Bass (*Dicentrarchus labrax*, L). PLoS ONE 7, e47957. https://doi.org/10.1371/journal.pone.0047957

Burgos-Aceves, M.A., Cohen, A., Smith, Y., Faggio, C., 2016. Estrogen regulation of gene expression in the teleost fish immune system. Fish Shellfish Immunol. 58, 42–49. https://doi.org/10.1016/j.fsi.2016.09.006
Chapman, J.C., Chapman, F.M., Michael, S.D., 2015. The production of alpha/beta and gamma/delta double negative (DN) T-cells and their role in the maintenance of pregnancy. Reprod. Biol. Endocrinol. 13. https://doi.org/10.1186/s12958-015-0073-5
Cheroutre, H., Lambolez, F., Mucida, D., 2011. The light and dark sides of intestinal intraepithelial lymphocytes. Nat. Rev. Immunol. 11, 445–456. https://doi.org/10.1038/nri3007
Chien, Y., Meyer, C., Bonneville, M., 2014. γδT Cells: First Line of Defense and Beyond. Annu. Rev. Immunol. 32, 121–155. https://doi.org/10.1146/annurev-immunol-032713-120216
Clark, D.A., 2016. The importance of being a regulatory T cell in pregnancy. J. Reprod. Immunol. 116, 60–69. https://doi.org/10.1016/j.jri.2016.04.288
Daley, S.R., Teh, C., Hu, D.Y., Strasser, A., Gray, D.H.D., 2017. Cell death and thymic tolerance. Immunol. Rev. 277, 9–20. https://doi.org/10.1111/imr.12532
del Pozo, A., Falcon, J., Sanchez-Vazquez, F.J., 2014. The Biological Clock and Dualism, in: Biology of European Sea Bass. CRC Press, pp. 34–56.
Do, Y., Ryu, S., Nagarkatti, M., Nagarkatti, P.S., 2002. Role of Death Receptor Pathway in Estradiol-Induced T-Cell Apoptosis in Vivo. Toxicol. Sci. 70, 63–72. https://doi.org/10.1093/toxsci/70.1.63
Dragin, N., Bismuth, J., Cizeron-Clairac, G., Biferi, M.G., Berthault, C., Serraf, A., Nottin, R., Klatzmann, D., Cumano, A., Barkats, M., Le Panse, R., Berrih-Aknin, S., 2016. Estrogen-mediated downregulation of AIRE influences sexual dimorphism in autoimmune diseases. J. Clin. Invest. 126, 1525–1537. https://doi.org/10.1172/JCI81894
Esteban, M.Á., Cuesta, A., Chaves-Pozo, E., Meseguer, J., 2015. Phagocytosis in Teleosts. Implications of the New Cells Involved. Biology 4, 907–922. https://doi.org/10.3390/biology4040907
Granja, A.G., Leal, E., Pignatelli, J., Castro, R., Abos, B., Kato, G., Fischer, U., Tafalla, C., 2015. Identification of Teleost Skin CD8 + Dendritic-like Cells, Representing a Potential Common Ancestor for Mammalian Cross-Presenting Dendritic Cells. J. Immunol. 195, 1825–1837. https://doi.org/10.4049/jimmunol.1500322
Green, T.J., Vergnes, A., Montagnani, C., de Lorgeril, J., 2016. Distinct immune responses of juvenile and adult oysters (*Crassostrea gigas*) to viral and bacterial infections. Vet. Res. 47, 72. https://doi.org/10.1186/s13567-016-0356-7
Guerreiro, P.M., Fuentes, J., Canario, A.V., Power, D.M., 2002. Calcium balance in sea bream (*Sparus aurata*): the effect of oestradiol-17beta. J. Endocrinol. 173, 377–385.
Hadidi, S., Glenney, G.W., Welch, T.J., Silverstein, J.T., Wiens, G.D., 2008. Spleen Size Predicts Resistance of Rainbow Trout to Flavobacterium psychrophilum Challenge. J. Immunol. 180, 4156–4165. https://doi.org/10.4049/jimmunol.180.6.4156
Hareramadas, B., Rai, U., 2006. Cellular mechanism of estrogen-induced thymic involution in wall lizard: caspase-dependent action. J. Exp. Zoolog. A Comp. Exp. Biol. 305A, 396–409. https://doi.org/10.1002/jez.a.260
Hince, M., Sakkal, S., Vlahos, K., Dudakov, J., Boyd, R., Chidgey, A., 2008. The role of sex steroids and gonadectomy in the control of thymic involution. Cell. Immunol. 252, 122–138. https://doi.org/10.1016/j.cellimm.2007.10.007
Jin, C., Fu, W.-X., Xie, L.-P., Qian, X.-P., Chen, W.-F., 2003. SDF-1α production is negatively regulated by mouse estrogen enhanced transcript in a mouse thymus epithelial cell line. Cell. Immunol. 223, 26–34. https://doi.org/10.1016/S0008-8749(03)00152-7
Klein, L., Kyewski, B., Allen, P.M., Hogquist, K.A., 2014. Positive and negative selection of the T cell repertoire: what thymocytes see (and don't see). Nat. Rev. Immunol. 14, 377–391.

https://doi.org/10.1038/nri3667
Lam, S.H., Chua, H.L., Gong, Z., Lam, T.J., Sin, Y.M., 2004. Development and maturation of the immune system in zebrafish, *Danio rerio*: a gene expression profiling, in situ hybridization and immunological study. Dev. Comp. Immunol. 28, 9–28. https://doi.org/10.1016/S0145-305X(03)00103-4
Lewis, K.L., Del Cid, N., Traver, D., 2014. Perspectives on antigen presenting cells in zebrafish. Dev. Comp. Immunol., Zebrafish Immunity and Infection Models 46, 63–73. https://doi.org/10.1016/j.dci.2014.03.010
Li, M.O., Rudensky, A.Y., 2016. T cell receptor signalling in the control of regulatory T cell differentiation and function. Nat. Rev. Immunol. 16, 220–233. https://doi.org/10.1038/nri.2016.26
Lin, J., Yang, L., Silva, H.M., Trzeciak, A., Choi, Y., Schwab, S.R., Dustin, M.L., Lafaille, J.J., 2016. Increased generation of Foxp3+ regulatory T cells by manipulating antigen presentation in the thymus. Nat. Commun. 7. https://doi.org/10.1038/ncomms10562
Lorin-Nebel, C., Budzinski, H., Le Ménach, K., Devier, M.H., Charmantier, G., Gros, R., Grousset, E., Blondeau-Bidet, E., Farcy, E., 2014. 4-Nonylphenol disrupts osmoregulation in the European sea-bass *Dicentrarchus labrax*. J. Xenobiotics 4. https://doi.org/10.4081/xeno.2014.4905
Lutton, B., Callard, I., 2006. Evolution of reproductive–immune interactions. Integr. Comp. Biol. 46, 1060–1071. https://doi.org/10.1093/icb/icl050
Luzio, A., Monteiro, S.M., Fontaínhas-Fernandes, A.A., Pinto-Carnide, O., Matos, M., Coimbra, A.M., 2013. Copper induced upregulation of apoptosis related genes in zebrafish (*Danio rerio*) gill. Aquat. Toxicol. 128–129, 183–189. https://doi.org/10.1016/j.aquatox.2012.12.018
Mañanós, E.L., Zanuy, S., Carrillo, M., 1997. Photoperiodic manipulations of the reproductive cycle of sea bass (*Dicentrarchus labrax*) and their effects on gonadal development, and plasma 17β-estradiol and vitellogenin levels. Fish Physiol. Biochem. 16, 211–222.
Manning, M.J., Nakanishi, T., 1996. The specific immune system: cellular defenses, in: The Fish Immune System: Organism, Pathogen, and Environment, Academic Press, Inc. pp. 159–205.
Martín, A., Alonso, L.M., Del Moral, M.G., Zapata, A.G., 1994. Ultrastructural changes in the adult rat thymus after estradiol benzoate treatment. Tissue Cell 26, 169–179. https://doi.org/10.1016/0040-8166(94)90092-2
Martín, A., Casares, F., Alonso, L., Nieuwenhuis, P., Vicente, A., Zapata, A.G., 1995a. Changes in the Blood-Thymus Barrier of Adult Rats after Estradiol-Treatment. Immunobiology 192, 231–248. https://doi.org/10.1016/S0171-2985(11)80100-2
Martín, A., Vicente, A., Torroba, M., Moreno, C., Jiménez, E., Zapata, A., 1995b. Increased numbers of CD5+ B cells in the thymus of estradiol benzoate-treated rats. Thymus 24, 111–127.
McCurley, A.T., Callard, G.V., 2008. Characterization of housekeeping genes in zebrafish: male-female differences and effects of tissue type, developmental stage and chemical treatment. BMC Mol. Biol. 9, 102. https://doi.org/10.1186/1471-2199-9-102
Mitter, K., Kotoulas, G., Magoulas, A., Mulero, V., Sepulcre, P., Figueras, A., Novoa, B., Sarropoulou, E., 2009. Evaluation of candidate reference genes for QPCR during ontogenesis and of immune-relevant tissues of European seabass (*Dicentrarchus labrax*). Comp. Biochem. Physiol. B Biochem. Mol. Biol. 153, 340–347. https://doi.org/10.1016/j.cbpb.2009.04.009
Muñoz-Ruiz, M., Sumaria, N., Pennington, D.J., Silva-Santos, B., 2017. Thymic Determinants of γδ T Cell Differentiation. Trends Immunol.

https://doi.org/10.1016/j.it.2017.01.007
Nakanishi, T., Shibasaki, Y., Matsuura, Y., 2015. T Cells in Fish. Biology 4, 640–663. https://doi.org/10.3390/biology4040640
Navas, J.M., Mañanós, E., Thrush, M., Ramos, J., Zanuy, S., Carrillo, M., Zohar, Y., Bromage, N., 1998. Effect of dietary lipid composition on vitellogenin, 17β-estradiol and gonadotropin plasma levels and spawning performance in captive sea bass (*Dicentrarchus labrax* L.). Aquaculture 165, 65–79. https://doi.org/10.1016/S0044-8486(98)00246-4
Nelson, E.R., Habibi, H.R., 2013. Estrogen receptor function and regulation in fish and other vertebrates. Gen. Comp. Endocrinol., 7th International Symposium on Fish Endocrinology 192, 15–24. https://doi.org/10.1016/j.ygcen.2013.03.032
Paiola, M., Knigge, T., Picchietti, S., Duflot, A., Guerra, L., Pinto, P.I.S., Scapigliati, G., Monsinjon, T., 2017. Oestrogen receptor distribution related to functional thymus anatomy of the European sea bass, *Dicentrarchus labrax*. Dev. Comp. Immunol. https://doi.org/10.1016/j.dci.2017.07.023
Pankhurst, N.W., Stacey, N.E., Peter, R.E., 1986. An evaluation of techniques for the administration of 17β-estradiol to teleosts. Aquaculture 52, 145–155. https://doi.org/10.1016/0044-8486(86)90034-7
Parra, D., Takizawa, F., Sunyer, J.O., 2013. Evolution of B Cell Immunity. Annu. Rev. Anim. Biosci. 1, 65–97. https://doi.org/10.1146/annurev-animal-031412-103651
Pfaffl, M.W., 2001. A new mathematical model for relative quantification in real-time RT–PCR. Nucleic Acids Res. 29, e45–e45. https://doi.org/10.1093/nar/29.9.e45
Pinto, P.I.S., Estêvão, M.D., Andrade, A., Santos, S., Power, D.M., 2016. Tissue responsiveness to estradiol and genistein in the sea bass liver and scale. J. Steroid Biochem. Mol. Biol. 158, 127–137. https://doi.org/10.1016/j.jsbmb.2015.12.023
Polanczyk, M.J., Carson, B.D., Subramanian, S., Afentoulis, M., Vandenbark, A.A., Ziegler, S.F., Offner, H., 2004. Cutting Edge: Estrogen Drives Expansion of the CD4+CD25+ Regulatory T Cell Compartment. J. Immunol. 173, 2227–2230. https://doi.org/10.4049/jimmunol.173.4.2227
Polanczyk, M.J., Hopke, C., Huan, J., Vandenbark, A.A., Offner, H., 2005. Enhanced FoxP3 expression and Treg cell function in pregnant and estrogen-treated mice. J. Neuroimmunol. 170, 85–92. https://doi.org/10.1016/j.jneuroim.2005.08.023
Quintana, F.J., Iglesias, A.H., Farez, M.F., Caccamo, M., Burns, E.J., Kassam, N., Oukka, M., Weiner, H.L., 2010. Adaptive Autoimmunity and Foxp3-Based Immunoregulation in Zebrafish. PLoS ONE 5, e9478. https://doi.org/10.1371/journal.pone.0009478
Rauta, P.R., Nayak, B., Das, S., 2012. Immune system and immune responses in fish and their role in comparative immunity study: A model for higher organisms. Immunol. Lett. 148, 23–33. https://doi.org/10.1016/j.imlet.2012.08.003
Rijhsinghani, A.G., Thompson, K., Bhatia, S.K., Waldschmidt, T.J., 1996. Estrogen blocks early T cell development in the thymus. Am. J. Reprod. Immunol. N. Y. N 1989 36, 269–277. https://doi.org/10.1111/j.1600-0897.1996.tb00176.x
Robinson, M.L., Gomez-Raya, L., Rauw, W.M., Peacock, M.M., 2008. Fulton's body condition factor K correlates with survival time in a thermal challenge experiment in juvenile Lahontan cutthroat trout (*Oncorhynchus clarki henshawi*). J. Therm. Biol. 33, 363–368. https://doi.org/10.1016/j.jtherbio.2008.05.004
Rodenas, M.C., Cabas, I., García-Alcázar, A., Meseguer, J., Mulero, V., García-Ayala, A., 2016. Selective estrogen receptor modulators differentially alter the immune response of gilthead seabream juveniles. Fish Shellfish Immunol. 52, 189–197. https://doi.org/10.1016/j.fsi.2016.03.041
Rodenas, M.C., Cabas, I., Gómez-González, N.E., Arizcun, M., Meseguer, J., Mulero, V., García-Ayala, A., 2017. Estrogens Promote the Production of Natural Neutralizing Antibodies

in Fish through G Protein-Coupled Estrogen Receptor 1. Front. Immunol. 8. https://doi.org/10.3389/fimmu.2017.00736
Rodewald, H.-R., 2008. Thymus Organogenesis. Annu. Rev. Immunol. 26, 355–388. https://doi.org/10.1146/annurev.immunol.26.021607.090408
Ross, M.A., Korenchevsky, V., 1941. The thymus of the rat and sex hormones. J. Pathol. Bacteriol. 52, 349–360.
Rotllant, J., Guerreiro, P.M., Anjos, L., Redruello, B., Canario, A.V.M., Power, D.M., 2005. Stimulation of Cortisol Release by the N Terminus of Teleost Parathyroid Hormone-Related Protein in Interrenal Cells *in Vitro*. Endocrinology 146, 71–76. https://doi.org/10.1210/en.2004-0644
Saltis, M., Criscitiello, M.F., Ohta, Y., Keefe, M., Trede, N.S., Goitsuka, R., Flajnik, M.F., 2008. Evolutionarily conserved and divergent regions of the Autoimmune Regulator (Aire) gene: a comparative analysis. Immunogenetics 60, 105–114. https://doi.org/10.1007/s00251-007-0268-9
Screpanti, I., Meco, D., Morrone, S., Gulino, A., Mathieson, B.J., Frati, L., 1991. In Vivo modulation of the distribution of thymocyte subsets: Effects of estrogen on the expression of different T cell receptor Vβ gene families in CD4−, CD8− thymocytes. Cell. Immunol. 134, 414–426. https://doi.org/10.1016/0008-8749(91)90314-2
Seemann, F., Knigge, T., Duflot, A., Marie, S., Olivier, S., Minier, C., Monsinjon, T., 2016. Sensitive periods for 17β-estradiol exposure during immune system development in sea bass head kidney: Sensitivity of sea bass head kidney development to E2. J. Appl. Toxicol. 36, 815–826. https://doi.org/10.1002/jat.3215
Seemann, F., Knigge, T., Olivier, S., Monsinjon, T., 2015. Exogenous 17-β-oestradiol (E2) modifies thymus growth and regionalization in European sea bass *Dicentrarchus labrax*. J. Fish Biol. 86, 1186–1198. https://doi.org/10.1111/jfb.12626
Segner, H., Verburg-van Kemenade, B.M.L., Chadzinska, M., 2017. The immunomodulatory role of the hypothalamus-pituitary-gonad axis: Proximate mechanism for reproduction-immune trade offs? Dev. Comp. Immunol. 66, 43–60. https://doi.org/10.1016/j.dci.2016.07.004
Steinman, R.M., Banchereau, J., 2007. Taking dendritic cells into medicine. Nature 449, 419–426. https://doi.org/10.1038/nature06175
Straub, R.H., 2007. The Complex Role of Estrogens in Inflammation. Endocr. Rev. 28, 521–574. https://doi.org/10.1210/er.2007-0001
Sugimoto, K., Hui, S.P., Sheng, D.Z., Nakayama, M., Kikuchi, K., 2017. Zebrafish FOXP3 is required for the maintenance of immune tolerance. Dev. Comp. Immunol. 73, 156–162. https://doi.org/10.1016/j.dci.2017.03.023
Szwejser, E., Verburg-van Kemenade, B.M.L., Maciuszek, M., Chadzinska, M., 2016. Estrogen-dependent seasonal adaptations in the immune response of fish. Horm. Behav. https://doi.org/10.1016/j.yhbeh.2016.10.007
Tai, P., Wang, J., Jin, H., Song, X., Yan, J., Kang, Y., Zhao, L., An, X., Du, X., Chen, X., Wang, S., Xia, G., Wang, B., 2008. Induction of regulatory T cells by physiological level estrogen. J. Cell. Physiol. 214, 456–464. https://doi.org/10.1002/jcp.21221
Teles, A., Thuere, C., Wafula, P.O., El-Mousleh, T., Zenclussen, M.L., Zenclussen, A.C., 2013. Origin of Foxp3+ cells during pregnancy. Am. J. Clin. Exp. Immunol. 2, 222–233.
Turchinovich, G., Pennington, D.J., 2011. T cell receptor signalling in γδ cell development: strength isn't everything. Trends Immunol. 32, 567–573. https://doi.org/10.1016/j.it.2011.09.005
Vandesompele, J., De Preter, K., Pattyn, F., Poppe, B., Van Roy, N., De Paepe, A., Speleman, F., 2002. Accurate normalization of real-time quantitative RT-PCR data by geometric averaging of multiple internal control genes. Genome Biol. 3, research0034–1.

https://doi.org/10.1186/gb-2002-3-7-research0034
Wan, F., Hu, C., Ma, J., Gao, K., Xiang, L., Shao, J., 2017. Characterization of γδ T Cells from Zebrafish Provides Insights into Their Important Role in Adaptive Humoral Immunity. Front. Immunol. 7. https://doi.org/10.3389/fimmu.2016.00675
Wang, C., Dehghani, B., Magrisso, I.J., Rick, E.A., Bonhomme, E., Cody, D.B., Elenich, L.A., Subramanian, S., Murphy, S.J., Kelly, M.J., Rosenbaum, J.S., Vandenbark, A.A., Offner, H., 2008. GPR30 Contributes to Estrogen-Induced Thymic Atrophy. Mol. Endocrinol. 22, 636–648. https://doi.org/10.1210/me.2007-0359
Wen, Y., Fang, W., Xiang, L.-X., Pan, R.-L., Shao, J.-Z., 2011. Identification of Treg-like cells in Tetraodon: insight into the origin of regulatory T subsets during early vertebrate evolution. Cell. Mol. Life Sci. 68, 2615–2626. https://doi.org/10.1007/s00018-010-0574-5
Wilson, A.B., 2017. MHC and adaptive immunity in teleost fishes. Immunogenetics 1–8. https://doi.org/10.1007/s00251-017-1009-3
Wira, C.R., Fahey, J.V., Abrahams, V.M., Rossoll, R.M., 2003. Influence of stage of the reproductive cycle and estradiol on thymus cell antigen presentation. J. Steroid Biochem. Mol. Biol. 84, 79–87. https://doi.org/10.1016/S0960-0760(03)00002-5
Yui, M.A., Rothenberg, E.V., 2014. Developmental gene networks: a triathlon on the course to T cell identity. Nat. Rev. Immunol. 14, 529–545. https://doi.org/10.1038/nri3702
Zha, J., Wang, Z., Wang, N., Ingersoll, C., 2007. Histological alternation and vitellogenin induction in adult rare minnow (*Gobiocypris rarus*) after exposure to ethynylestradiol and nonylphenol. Chemosphere 66, 488–495. https://doi.org/10.1016/j.chemosphere.2006.05.071
Zoller, A.L., Kersh, G.J., 2006. Estrogen Induces Thymic Atrophy by Eliminating Early Thymic Progenitors and Inhibiting Proliferation of -Selected Thymocytes. J. Immunol. 176, 7371–7378. https://doi.org/10.4049/jimmunol.176.12.7371
Zoller, A.L., Schnell, F.J., Kersh, G.J., 2007. Murine pregnancy leads to reduced proliferation of maternal thymocytes and decreased thymic emigration. Immunology 121, 207–215. https://doi.org/10.1111/j.1365-2567.2006.02559.x
Žuklys, S., Handel, A., Zhanybekova, S., Govani, F., Keller, M., Maio, S., Mayer, C.E., Teh, H.Y., Hafen, K., Gallone, G., Barthlott, T., Ponting, C.P., Holländer, G.A., 2016. Foxn1 regulates key target genes essential for T cell development in postnatal thymic epithelial cells. Nat. Immunol. 17, 1206–1215. https://doi.org/10.1038/ni.3537
Zwollo, P., 2016. The humoral immune system of anadromous fish. Dev. Comp. Immunol. https://doi.org/10.1016/j.dci.2016.12.008

Figure and Tables

Table 1: Experimental and physicochemical conditions with somatic indices for each experimental group (for detail and experimental setup see text and supplementary materials and methods). Values are means and standard deviation (s.d.). GSI, gonado-somatic index; HSI, hepato-somatic index; *K,* Fulton's condition factor; SSI, spleno-somatic index.

Tank volume	1,800 L					
Water flow	continuous					
Exposure route	intraperitoneal injection					
E2 doses	0.5 mg/kg injected 3 times					
Exposure duration	1 week					
Physicochemical conditions	November 2014 (Experiment 1)					
	CTR		s.d.	E2		s.d.
Temperature (°C)	13.70	±	0.26	13.67	±	0.18
pH	8.13	±	0.52	8.16	±	0.11
Conductivity (mS/cm)	46.54	±	5.96	47.36	±	4.03
Salinity (g/kg)	30.65	±	3.19	32.09	±	0.78
Fish density per tank g/L	7.35			7.52		
Somatic indices						
K	1.32	±	0.11	1.36	±	0.11
GSI	0.50	±	0.31	0.601	±	0.62
SSI	0.10	±	0.04	0.09	±	0.03
HSI	1.21	±	0.27	1.29**	±	0.35
Physicochemical conditions	December 2014 (Experiment 2)					
	CTR		s.d.	E2		s.d.
Temperature (°C)	11.58	±	0.58	11.92	±	0.46
pH	8.68	±	0.58	8.84	±	0.67
Conductivity (mS/cm)	37.55	±	0.53	38.07	±	0.48
Salinity (g/kg)	32.98	±	0.07	33.16	±	0.19
Fish density per tank g/L	9.12			8.80		
Somatic indices						
K	1.41	±	0.21	1.36	±	0.11
GSI	0.74	±	0.65	1.02	±	1.14
SSI	0.11	±	0.03	0.09	±	0.03
HSI	1.52	±	0.34	1.68 ✢	±	0.32

** and ✢, significantly different between CTR- and E2-groups of the respective experiment at p≤0.001 (*t*-test or *U*- test, respectively)

Table 2: Sample sizes analysed in each treatment group. GSI, gonado-somatic index; HSI, hepato-somatic index; *K,* Fulton's condition factor; SSI, spleno-somatic index.

Biometric index	CTR-F	E2-F	CTR-M	E2-M
K	59	55	18	22
GSI	59	54	18	21
SSI	30	27	10	13
HSI	59	55	18	22
Gene expression				
Thymus	15	13	5	7
Head-kidney	14	11	9	11
Spleen	12	11	10	8
Plasmatic parameters				
E2	26	25	9	10
VTG	8	12	7	6
Ca	26	24	9	10
P_i	26	23	9	10
Cortisol	26	25	9	11
Flow cytometry				
Head-kidney	10	9	5	6
Spleen	7	4	4	5

Table 3: Matrices of Spearman Rank Order correlations between the plasmatic E2-, cortisol- and gene-expression levels in control (CTR-F) and E2-injected females (E2-F) in the thymus (T), the head-kidney (HK) and the spleen (S). Significantly positive correlations (p<0.004) are marked as green, chequered squares. Yellow, dotted squares signify insufficient replicate number (n≤5) and, therefore, absence of correlation. Redundant data are depicted as shaded squares. Casp, Caspase; other abbreviations as in text.

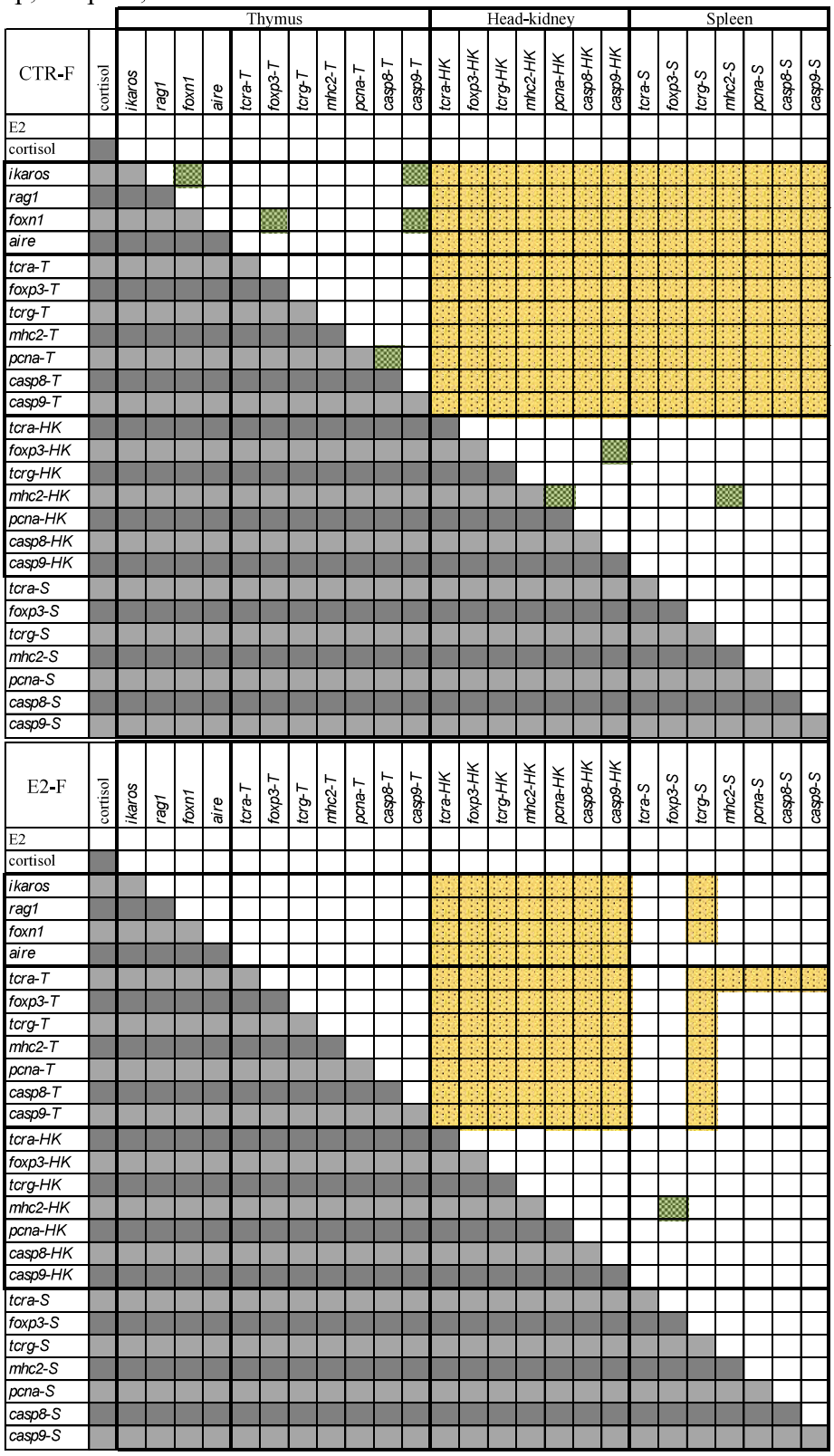

Table 4: Matrices of Spearman Rank Order correlations between the plasmatic E2-, cortisol- and gene-expression levels in control (CTR-M) and E2-injected males (E2-M) in the thymus (T), the head-kidney (HK) and the spleen (S). Significantly positive correlations (p<0.004) are marked as green, chequered squares. Yellow, dotted squares signify insufficient replicate number (n≤5) and, therefore, absence of correlation. Redundant data are depicted as shaded squares. Casp, Caspase. Caspase; other abbreviations as in text.

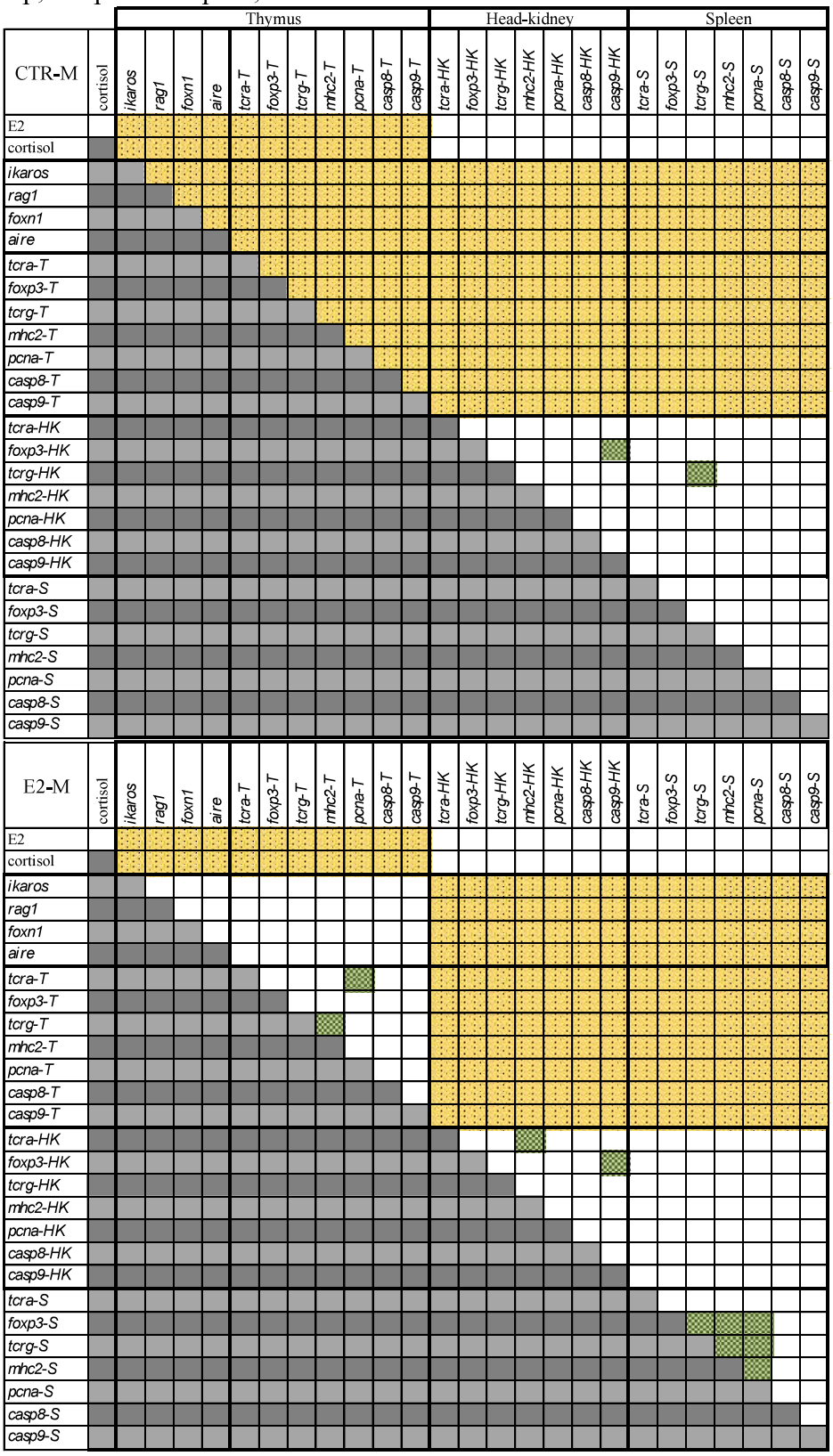

Figure legends

Fig. 1: Successive steps of teleost thymic and peripheral T cell differentiation in steady-state associated with their corresponding genetic markers used in the present study. **1**, The head-kidney (bone marrow equivalent) contains hematopoietic stem cells providing both myeloid and lymphoid progenitors (Boehm and Swann, 2014; Parra et al., 2013). The common lymphoid progenitor (CLP) differentiates into the B cell lineage or migrates to the thymus. **2 A**, Following homing, early thymic progenitor (ETP) commit to the T cell lineage after interacting with thymic epithelial cells (TEC) (Bajoghli et al., 2009; Yui and Rothenberg, 2014). **2 B**, TCR gene recombination determines the immature T cell fate: apoptosis (death by neglect) or αβ and γδ T cell differentiation following β or γδ selection. Committed αβ T cells undergo positive selection, resulting in CD4 or CD8 SP differentiation (Klein et al., 2014; Muñoz-Ruiz et al., 2017; Turchinovich and Pennington, 2011). **2 C**, selected αβ T cells can undergo negative selection or Treg differentiation, two processes important for central tolerance. Negative selection allows the elimination of potentially harmful autoreactive T cells with a high TCR affinity for the self-peptide-MHC complex by apoptosis (Klein et al., 2014; Li and Rudensky, 2016). **3**, Naïve and mature T cells migrate into the secondary lymphoid organs, where they undergo a new selection process important for peripheral tolerance, including clonal selection and Treg differentiation (Audiger et al., 2017; Li and Rudensky, 2016). The selected self-tolerant T cells constitute a pool of immunocompetent T cells able to elaborate and coordinate a specific immune response (Boehm and Swann, 2014; Nakanishi et al., 2015).

Fig. 2: Circulating plasma levels of 17β-oestradiol (E2), cortisol, calcium (Ca^{2+}), inorganic phosphorus (P_i) and vitellogenin (Vtg) in sea bass, *Dicentrarchus labrax*, observed in females (F) and males (M) of E2-exposed (E2) and control (CTR) fish. Circulating plasma levels are represented by box-and-whisker plots. The horizontal line inside each box indicates the median, top lines of the box are the 25 and 75 percentiles and the whisker limits represent extreme values. Asterisks indicate significant differences between the E2 and CTR group at the level *, $0.05 \geq p > 0.01$ and ***, $p < 0.001$, respectively (Mann-Whitney *U*-test).

Fig. 3: Relative expression of thymic function-related genes, *ikaros, rag1*, *foxn1* and *aire*, in the thymus of sea bass, *Dicentrarchus labrax*, in females (F) and males (M) of E2-exposed (E2) and control (CTR) fish. Relative expression-levels are represented by box-and-whisker plots. The horizontal line inside each box indicates the median, top lines of the box are the 25 and 75 percentiles and the whisker limits depict extreme values. *, significantly different at $p=0.007$ (Mann-Whitney *U*-test)

Fig. 4: Relative expression of antigen-presenting cell and cellular homeostasis-related genes, *mhc2a, caspase8*, *caspase9* and *pcna*, in thymus, head-kidney and spleen of sea bass, *Dicentrarchus labrax*, in females (F) and males (M) of E2-exposed (E2) and control (CTR) fish. Relative expression-levels are represented by box-and-whisker plots with the median, 25 % and 75 % quartiles as well as extreme values depicted by the bars. *, significantly different at $p=0.038$ (*t*-test)

Fig. 5: Relative expression of T cell-related genes, *tcra*, *foxp3* and *tcrg*, in thymus, head-kidney and spleen of sea bass, *Dicentrarchus labrax*, in females (F) and males (M) of E2-exposed (E2) and control (CTR) fish. Relative expression-levels are represented by box-and-whisker plots with the median, 25 % and 75 % quartiles as well as extreme values depicted by the bars. Asterisks indicate significant differences at $p<0.05$ (*, *U*-test, *, *t*-test).

Fig. 6: Flow cytometric analysis of sea bass leucocytes isolated from the head-kidney (HK) and spleen (S) of control (CTR) and E2-exposed (E2) fish. a, side scatter (SSC) / Electronic volume (EV) profiles with the gates for lymphoid (Ly) and myeloid cells (My) for each organ; b, leucocyte mortality and distribution; c, ROS-levels of stimulated and unstimulated cells, *i.e.*, with and without PMA, respectively, depicted as Mean Fluorescent Intensity (MFI); d, Respiratory Burst Index. Values are means ± standard error. Asterisks indicate significant differences between control and E2-treated fish at *, $p<0.05$, (*U*-test) and *, $p=0.02$ (*t*-test).

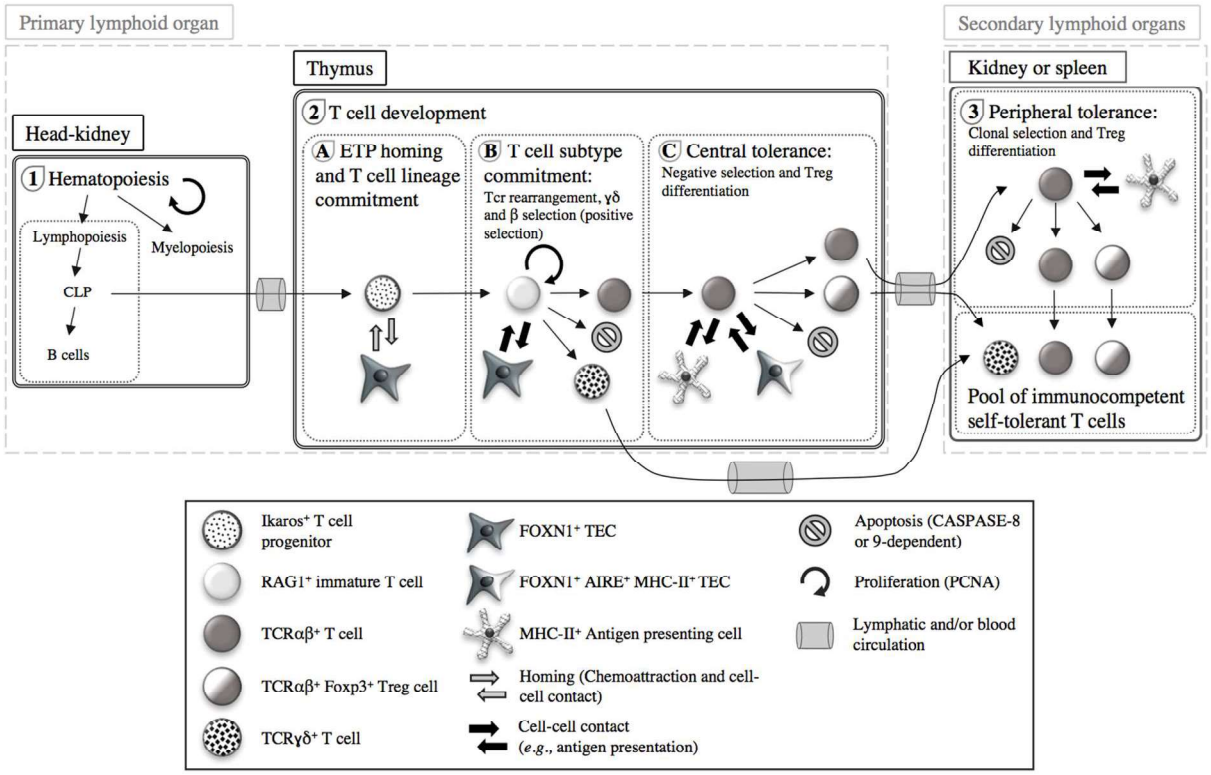

Figure 1

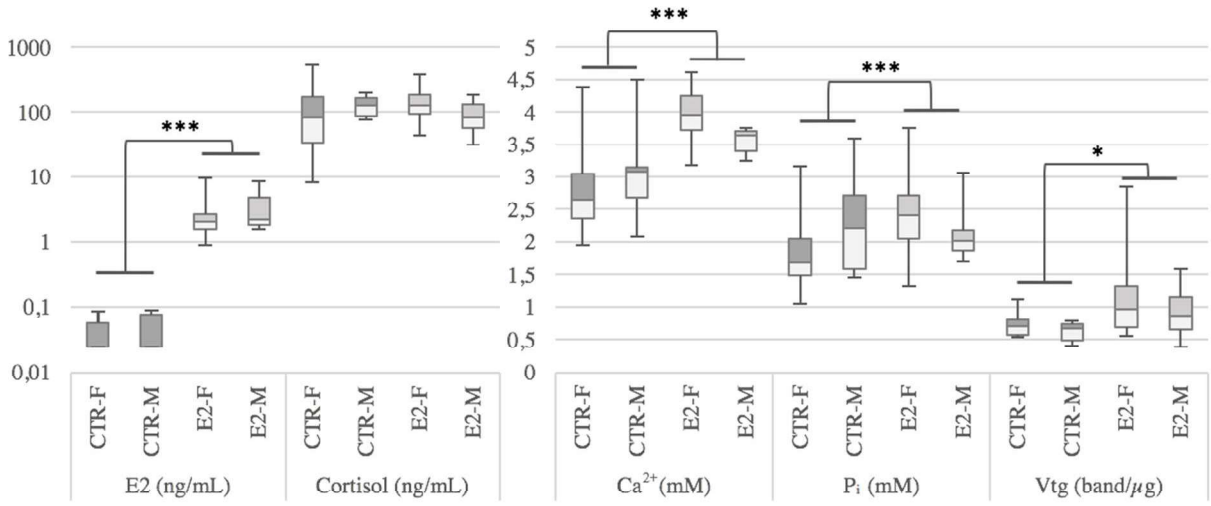

Figure 2

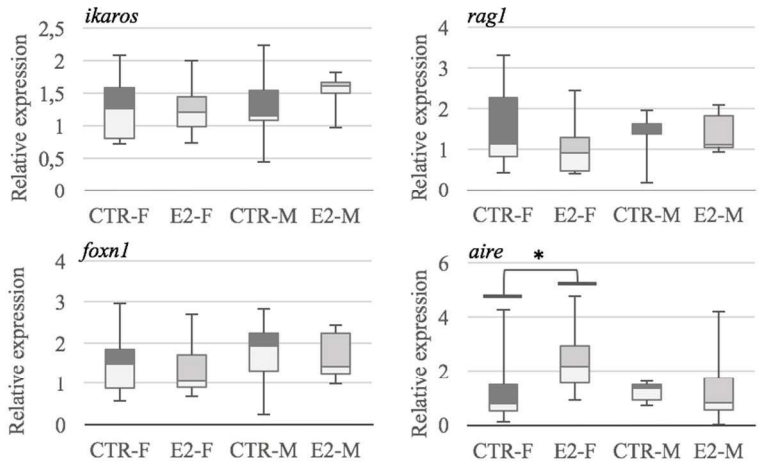

Figure 3

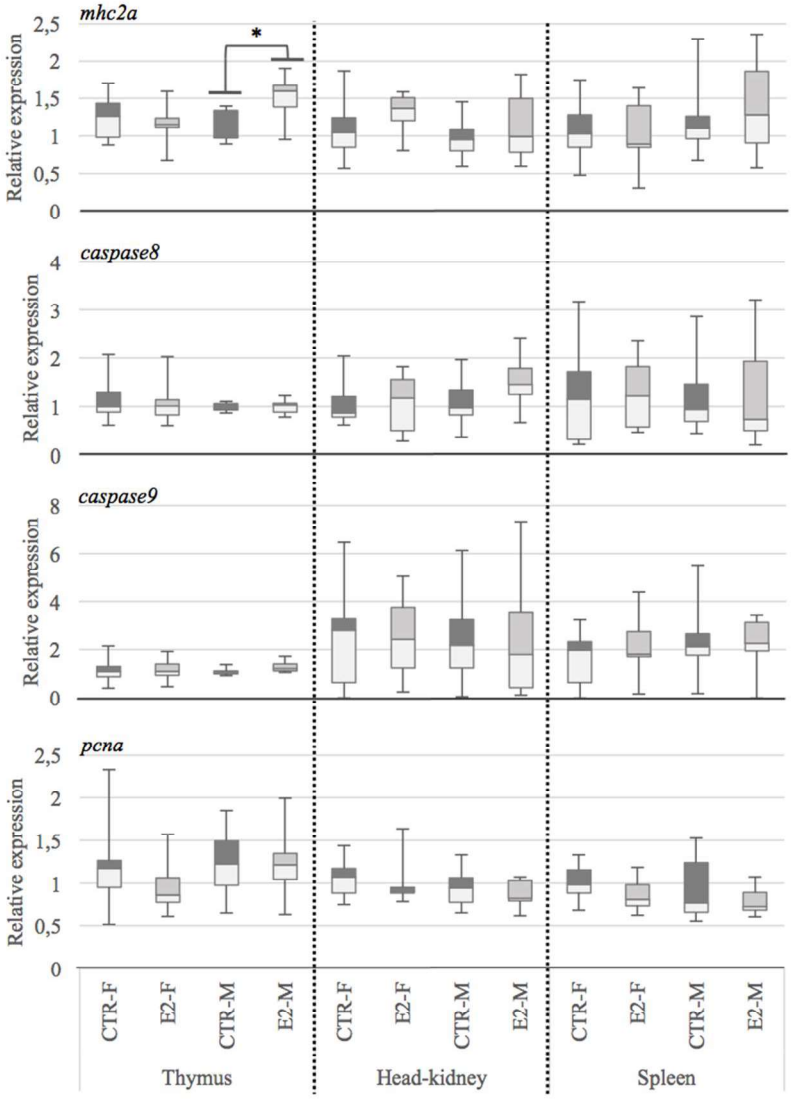

Figure 4

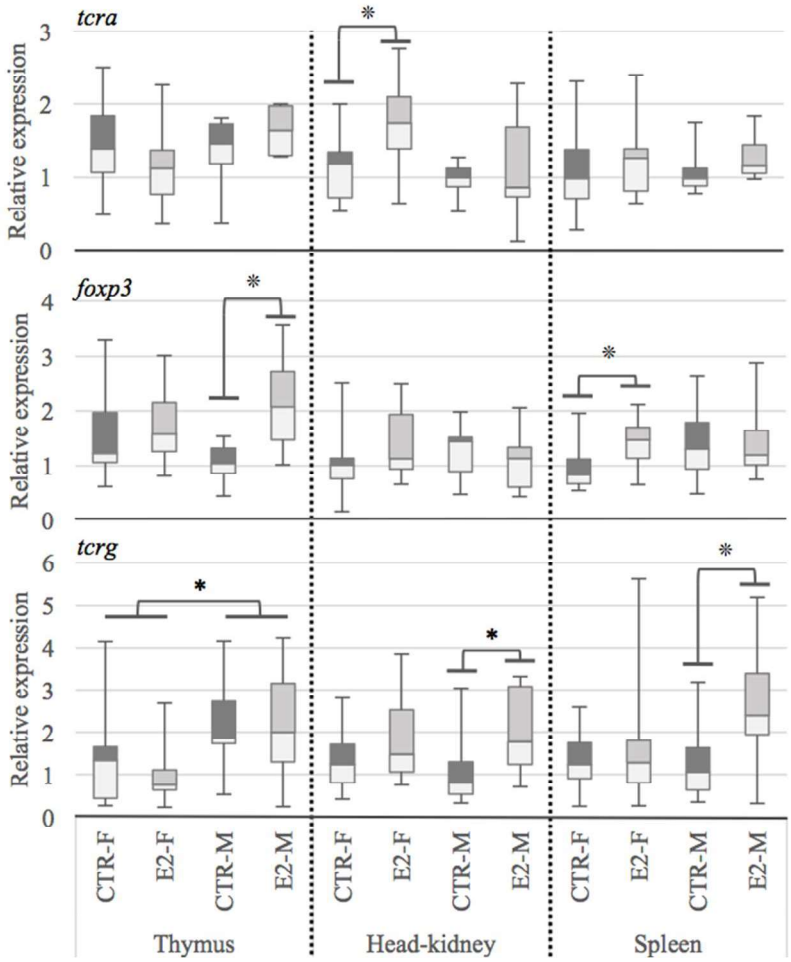

Figure 5

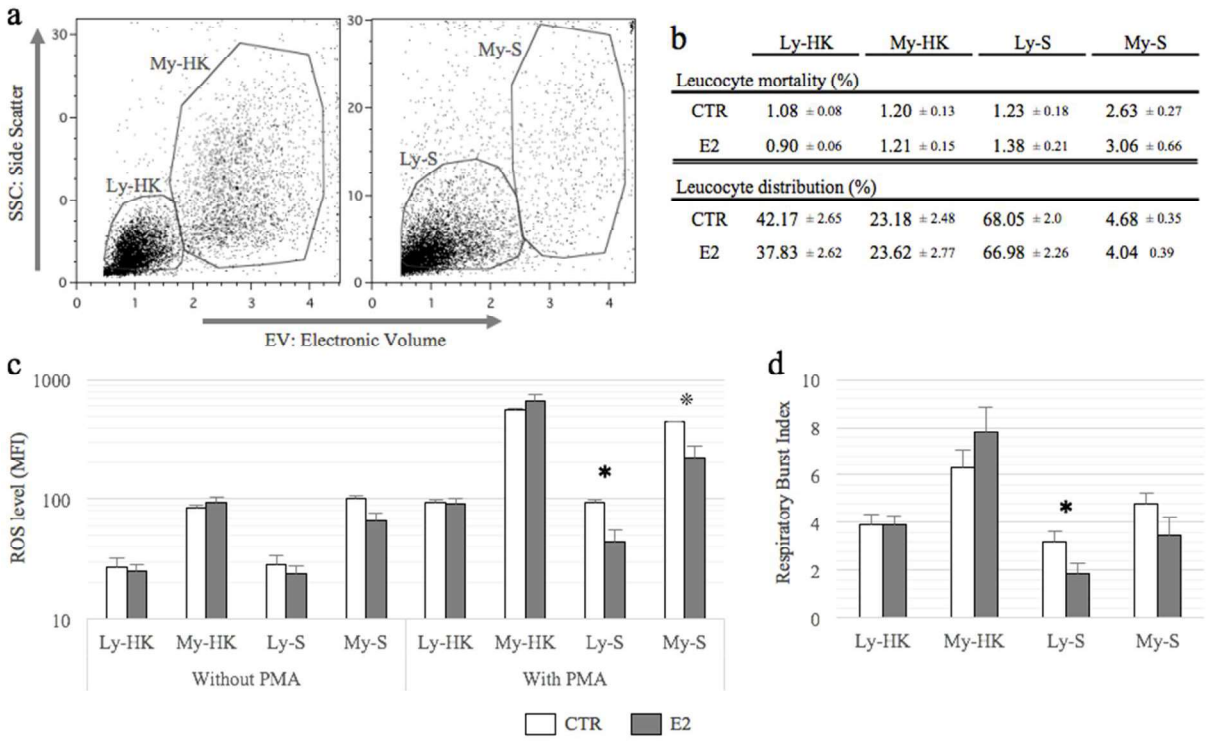

Figure 6

Supplementary data

A-Materials and Methods:

E2 solution preparation: E2-solutions of 0.5 mg/mL, 1 mg/mL and 2mg/mL were freshly prepared before each experiment, allowing for minimal volumes to be injected. Briefly, 17β-oestradiol (E8875; Sigma) was dissolved at 50 mg/mL in absolute ethanol, dispersed in organic colza oil (La Vie Claire, Montagny, France) and incubated overnight in obscurity at 30 °C to evaporate the solvent. The vehicle control was prepared in exactly the same way, but without E2. During each experiment, the solutions were conserved in obscurity at 4 °C.

Statistical analysis: Eight experimental groups were analysed in this study (Figure S1), divided in control (CTR) or exposed (E2) females (F) and males (M) from the experiment of November (1) and December (2) (*i.e.*, CTR-F-1, CTR-F-2, E2-F-1, E2-F-2, CTR-M-1, CTR-M-2, E2-M-1 and E2-M-2). To evaluate if these experimental groups could be combined, a Kruskal-Wallis rank sum-test was applied to compare the different biometric indices (*K,* GSI, SSI and HSI) and the plasmatic levels of cortisol, E2, Ca^{2+}, P_i and Vtg between the eight experimental groups, followed by a Tukey-Kramer (Nemenyi) *post-hoc* test (Figure S1). Overall sample size analysis can be consulted in Table 1 and number of individuals per group in Figure S1. The biometric indices and the plasmatic parameters were compared between the males and females of both treatment groups (E2-F, CTR-F, E2-M and CTR-M) from both experiments. Furthermore, E2- and CTR-groups were combined to detect possible gender differences. For pairwise analysis, if normal distribution and homoscedasticity could be confirmed, an independent Student *t*-test was used for parametric hypothesis testing; otherwise non-parametric Mann-Whitney *U*-test was conducted.

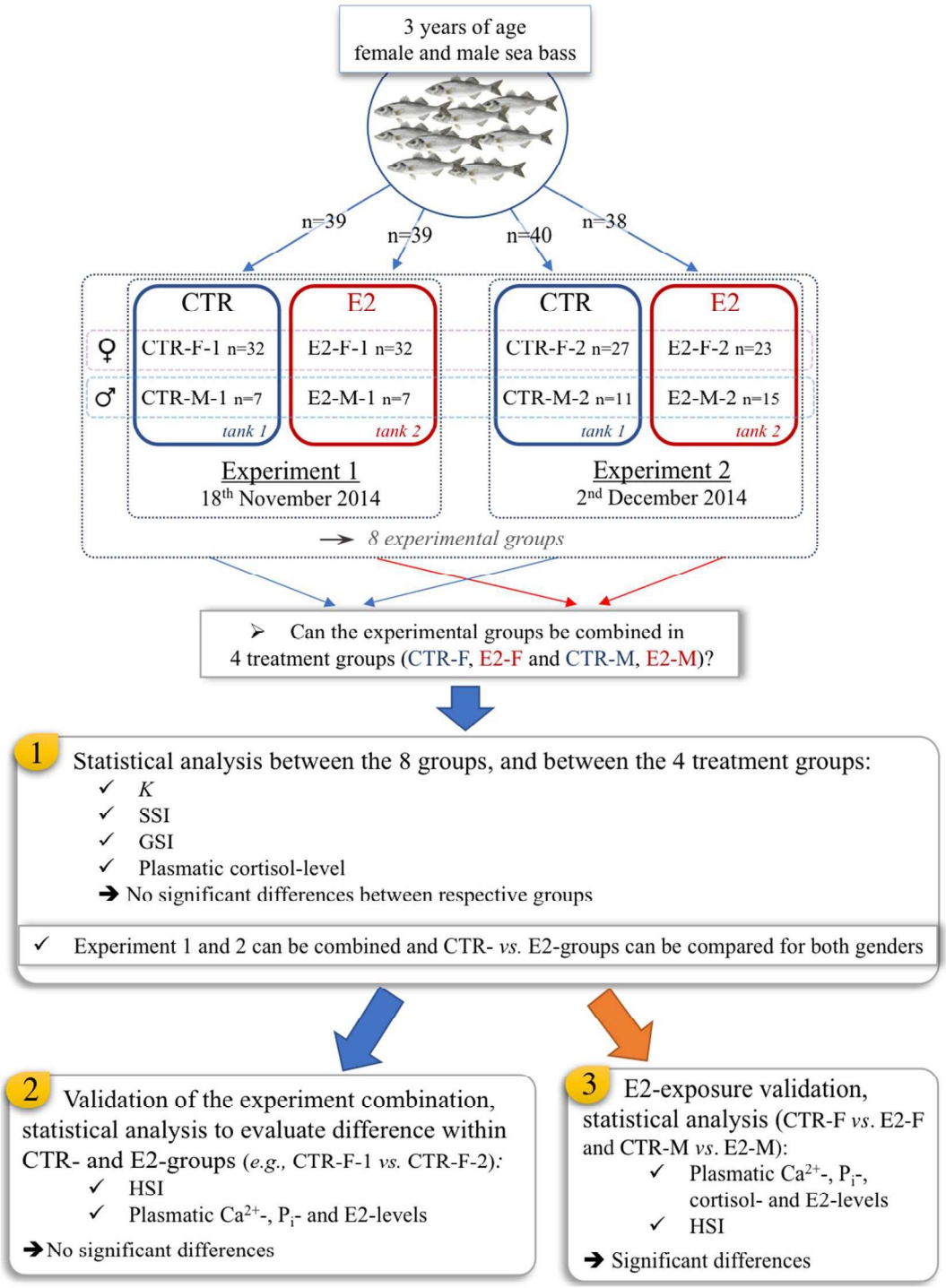

Figure S1: Experimental setup and procedure to validate the pooling of the two experiments. Two successive E2-exposures were conducted leading to 8 experimental groups corresponding to the control and treated fish from both genders and both experiments, i.e., CTR-F-1, CTR-F-2, E2-F-1, E2-F-2, CTR-M-1, CTR-M-2, E2-M-1 and E2-M-2. (1) To validate that both experiments can be combined in four treatment groups including the control and treated groups of both genders (CTR-F, E2-F, CTR-M and E2-M), Fulton's condition factor (K), spleno-somatic index (SSI), gonado-somatic index (GSI) and plasmatic cortisol-level were compared. Because no statistically significant difference could be detected when comparing between the treatment groups for both sexes, the experiments were combined. As a confirmation, (2) no statistically significant differences were observed when comparing: the hepato-somatic index (HSI) and the plasmatic level of Ca^{2+}, P_i and E2 between the respective treatment groups. Subsequently, (3) the E2-exposure was validated with both experiments combined using the plasmatic Ca^{2+}-, P_i- and cortisol-levels as well as the HSI. The different groups were compared using a Kruskal-Wallis rank sum-test followed by a Tukey-Kramer (Nemenyi) post-hoc test.

Table S1: Sample sizes analysed in each experimental group.

Experiment 1 (November 2014)					Experiment 2 (December 2014)				
Biometric index	CTR-F-1	CTR-M-1	E2-F-1	E2-M-1	Biometric index	CTR-F-2	CTR-M-2	E2-F-2	E2-M-2
K	32	7	32	7	*K*	27	11	23	15
GSI	32	7	32	7	GSI	27	11	22	14
SSI	16	4	16	4	SSI	14	6	11	9
HSI	32	7	32	7	HSI	27	11	23	15
Gene expression					Gene expression				
Thymus	6	2	7	2	Thymus	9	3	6	5
Head-kidney	8	4	6	4	Head-kidney	6	5	5	7
Spleen	8	4	6	3	Spleen	4	6	5	5
Plasmatic parameters					Plasmatic parameters				
E2	13	3	13	3	E2	13	6	12	7
VTG	4	2	7	2	VTG	4	5	5	4
Ca	13	3	13	3	Ca	13	6	11	7
P_i	13	3	12	3	P_i	13	6	11	7
Cortisol	13	3	13	3	Cortisol	13	6	12	8
Flow cytometry					Flow cytometry				
Head-kidney	4	2	4	2	Head-kidney	6	3	5	4
Spleen	4	2	3	2	Spleen	4	1	1	3

Partial gene sequences determination: For *foxn1* and *ikaros* transcript quantification, we first designed primers for conserved sequences by multi-sequence alignments of the following sequences: *Danio rerio*, Accession no. AF092175.1; *Homo sapiens*, BC018349.1; *Xenopus tropicalis,* 001015698.1; *Gallus gallus,* 205088.1; *Larimichtys crocea*, 010734525.1 ; *Salmo salar*, 001173899.1 for *ikaros* and *Larimichthys crocea,* 010735826.1; *Danio rerio,* 212573.1, *Oryzias latipes,* AB274724.1, *Stegastes partitus,* 008295040.1, *Poecilia Formosa,* 007563077.1 for *foxn1*. Partial gene sequences of *D. labrax ikaros* and foxn1 were amplified using the primers specific for the conserved parts of the sequence (Table S2). PCR was performed with cDNA from the thymus of sea bass, specific primers and the Purple Taq (Ozyme, Montigny-le-Bretonneux, France). Negative controls were performed with DNA free water. PCR conditions were as follows: initial incubation at 95°C for 2min followed by 72°C for 5min. For all genes, 40 cycles at 95° for 30s, 60° for 30s (the hybridization temperature is primer specific, see Table S2) and 72°C for 45s were carried out for the Purple Taq. The size of the various amplicons was determined on 2% agarose gels. The PCR product were purified using the Wizard® SV Gel and PCR Clean-Up System (Promega, Fitchburg, USA) and following the manufacturer instructions. Purified PCR products were then sequenced to validate the amplification specificity and to design specific primers for qPCR (Table S3).

* decrease of 1°C at each cycle over 10 consecutive cycles followed by constant hybridation temperature.

Table S2: Oligonucleotide sequences used to amplify and sequence partial D. labrax sequences

Genes	Primers 5'-3'	Amplicon pb	Hybridation Temperature
foxn1	F: GCATCTTGATCTTCTTGGCTCTG R: CCACTTGTGCAGCTCCTCC	260	60°C
ikaros	F: AGTGTGGTGCCTCTTTCACC R: TCTGTGGCATAGTGCTCTTAC	396	70°C*

Table S3: Oligonucleotide sequences and qPCR conditions for the selected thymic function-related genes (ikaros, rag1, foxn1 and aire), homeostasis-related genes (caspase8, caspase9 and pcna) as well as antigen-presenting-cell- and T cell-related genes (mhc2a, tcra, foxp3 and tcrg). Normalised relative gene expression was calculated by geometric means (for details see text) using three reference genes (ef1a, l13a, fau).

Genes	Primers 5'-3'	Amplicon pb	Hybridation Temperature	Amount of Primer	Reaction volume qPCR	Efficiency			Gene accession numbers
						Thymus	HK	Spleen	
ikaros	F: TTTCACCCAGAAGGGCAACC R: CCGAATGGGTGCGTAAATGG	131	57.5°C	0.5 µM	10 µL	1.97			DLAgn_000 10890
rag1	F: CACTGGCTCTACACCTCCAA R: CTCATCTTCCAGGCTCTCCAC	108	60°C	0.75 µM	5 µL	1.98			AF137181.1
foxn1	F: CCCTATCTACAGCACCACCT R: GAATAGTGTGGACGGCGAAT	84	60°C	0.5 µM	5 µL	2.00			DLAgn_000 31910
aire	F: ACGTCGGTGGGGAGTTTTAC R: TCCGTCCTTACACACTGCAC	158	60°C	0.5 µM	5 µL	2.18			DLAgn_561 0
tcra	F: GGCCACTGGTTTCAGCAGAT R: AGAGCCATGAGGTTCACCAT	213	60°C	0.5 µM	1.5 µL	1.99	1.99	1.90	AY831387. 1
foxp3	F: GGAGCAGTATTGTGGGCACT R: TCGTCTGGAAGCTGTTTGGG	80	60°C	0.5 µM	1.5 µL	1.99	1.83	2.10	KJ818328
tcrg	R: CCAACTGCACACATGCTGAC R: TTGAGGCACTTTATCAAACCTGT	164	60°C	0.5 µM	10 µL	1.96	1.94	1.97	EU853841.1
pcna	F: GCTGGGTACAGGAAACGTCA R: GCGTGGCTTTGGTGAAGAAG	137	60°C	0.5 µM	1.5 µL	1.919	1.98	1.77	JQ755266.1
mhc2a	F: GGTCTGACTGTCGGTCTGCT R: TGCACTCGTTTCCTTTGATG	67	60°C	0.5 µM	1.5 µL	2.04	1.98	1.90	AM113466. 1
caspase8	F: TGTCAGGGAAGCCTCTACCA R: CATCCCCAGCAGGAAGTCAG	150	60°C	0.5 µM	5 µL	2.28	1.98	2.00	FJ225665.1
caspase9	F: CGAATGCAACCGAGCACAAA R: ACTAACGACCGCCAATGAGG	193	60°C	0.5 µM	5 µL	2.09	2.13	1.80	DQ345775. 1
l13a	F: TCTGGAGGACTGTCAGGGGCATGC R: AGACGCACAATCTTGAGAGCAG	145	60°C	0.5 µM	1.5 µL	2.08	2.10	2.04	DLAgn_000 23060
fau	F: GACACCCAAGGTTGACAAGCAG R: GGCATTGAAGCACTTAGGAGTTG	149	60°C	0.5 µM	1.5 µL	1.96	2.04	1.97	DLAgn_000 67980
ef1a	F: GGCTGGTATCTCTAAGAACG R: CCTCCAGCATGTTGTCTCC	239	60°C	0.5 µM	1.5 µL	1.60	2.00	2.03	AJ866727.1

B-Results:

Female and male fish had total lengths of 30.07 cm ± 2.16 s.d. and 29.72 cm ± 2.25 s.d., respectively, and weighed 377.4 g ± 87.63 s.d. and 380.9 g ± 97.82 s.d.. When comparing the biometric indices between all eight experimental groups (see figure S2), the Fulton's condition factor *K* indicated significant differences between the experimental groups (*Kruskal-Wallis*, $H_{7,146}=20.35$, p=0.005). The *post-hoc* analysis revealed a significant difference between CTR-F-1 and E2-M-2 (p=0.021) and between CTR-M-1 and E2-M-2 (p=0.010) (overall p-values are reported in Table S4). The GSI (*Kruskal-Wallis*, $H_{7,146}$=7.87, p=0.344) did not differ significantly across all experimental groups, neither did the SSI (*Kruskal-Wallis*, $H_{7,72}$=9.06, p=0.248), nor the plasmatic level of cortisol (*Kruskal-Wallis*, $H_{7,63}$=13.27, p=0.066).

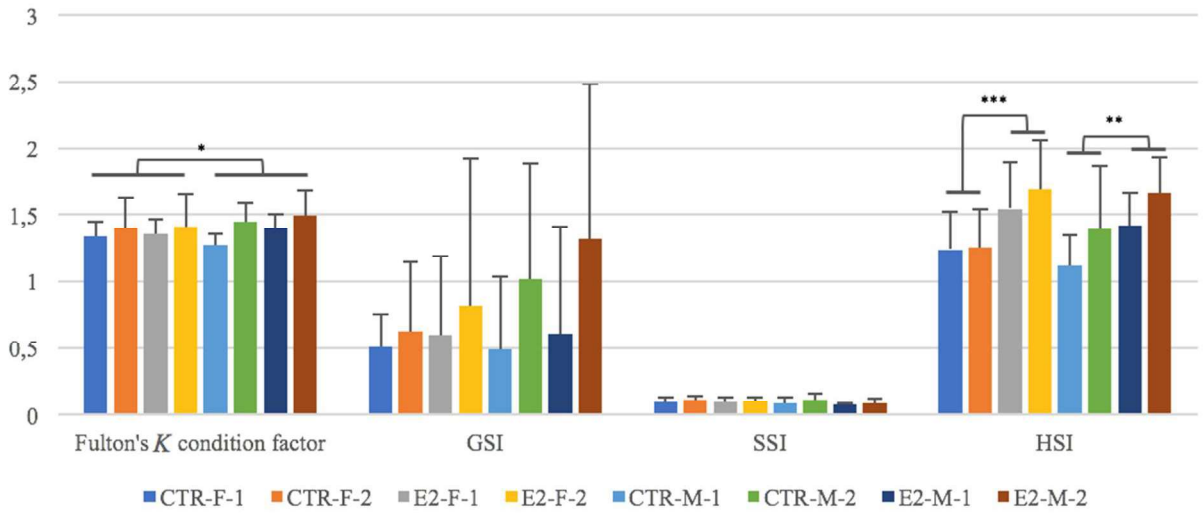

*Figure S2: Biometric indices (Fulton's K condition factor, gonado-somatic index (GSI), spleno-somatic index (SSI) and hepato-somatic index (HSI)) of the different experimental groups including control (CTR), exposed (E2), females (F) and males (M) from the experiment of November (1) and December (2). Indices are means and standard deviation. *, significantly different at 0.05≥p>0.01 for males and females from both experiments and treatments combined; **, significantly different at 0.01≥p>0.001 for males from both experiments combined and ***, significantly different at p<0.001 for females from both experiments combined.*

Table S4: p-values obtained with the Tukey-Kramer (Nemenyi) post-hoc test corresponding to the Fulton's condition factor K pairwise analysis of the experimental groups. Values indicate significant differences at p<0.05

	CTR-F-1	CTR-F-2	CTR-M-1	CTR-M-2	E2-F-1	E2-F-2	E2-M-1
CTR-F-2	0.974						
CTR-M-1	0.861	0.492					
CTR-M-2	0.299	0.804	0.082				
E2-F-1	0.994	1.000	0.584	0.662			
E2-F-2	0.818	1.000	0.304	0.961	0.994		
E2-M-1	0.878	0.997	0.387	1.000	0.987	0.999	
E2-M-2	0.021	0.237	0.010	1.000	0.123	0.547	0.970

When both experiments were combined to compare females and males from the two treatment groups (CTR *vs*. E2), *K* values were significantly different (*Kruskal-Wallis*, $H_{3,150}$=9.53, p=0.023), with *post-hoc* analysis revealing a significant difference between CTR-F and E2-M (p=0.011; overall p-values are listed in Table S5). When combining the two experiments, the GSI (*Kruskal-Wallis*, $H_{3,150}$=0.87, p=0.832), the SSI (*Kruskal-Wallis*, $H_{3,74}$=0.87, p=0.198) and the plasmatic level of cortisol (*Kruskal-Wallis*, $H_{3,67}$=5.81, p=0.121; Fig. 2) did not reveal any significant difference between CTR-F, CTR-M, E2-F and E2-M.

Table S5: p-values obtained with the Tukey-Kramer (Nemenyi) post-hoc test corresponding to the Fulton's K condition factor pairwise analysis with the two experiments confounded. Values in red correspond to p<0.05

	CTR-F	CTR-M	E2-F
CTR-M	0.951		
E2-F	0.824	1.000	
E2-M	0.011	0.203	0.077

Comparing E2 *vs*. CTR with all inviduals, *i.e.*, both genders and both experiments combined, *K* (*U*-test, p=0.062), GSI (*U*-test, p=0.380), SSI (*U*-test, p=0.092) and cortisol-levels (*U*-test, p=0.367) were not statistically different.

Fish from control and treatment groups of the two experiments combined, revealed a significant difference between the *K* of females with 1.37 g/cm^3 ± 0.18 s.d., which was slightly lower than that of males, 1.42 g/cm^3 ± 0.17 s.d. (*U*-test, p=0.026). The GSI between males and females, all treatment groups and both experiments confounded, was not statistically different (*U*-test, p=0.380), neither was the SSI (*U*-test, p=0.092), nor the cortisol-level (*U*-test, p=0.578).

Considering the plasmatic E2-levels in all eight experimental groups, the statistical analysis revealed significant differences (*Kruskal-Wallis*, $H_{7,60}$=54.07, p<0.001), in the HSI values (*Kruskal-Wallis*, $H_{7,146}$=44.94, p<0.001) as well as in the plasmatic level of Ca^{2+} (*Kruskal-Wallis*, $H_{7,61}$=39.10, p<0.001). The *post-hoc* analysis indicated a significant difference of E2-levels, HSI and Ca^{2+}-levels between the CTR and the E2 group for all pairs, except the males of the first experiment (see p-values in Table S6-8). Considering the plasmatic level of P_i, the statistical analysis with all experimental groups revealed a significant difference (*Kruskal-Wallis*, $H_{7,61}$=39.10, p=0.011), with the *post-hoc* analysis indicating a significant difference between CTR and E2 group for female of the second experiment only (see p value in Table S9).

Table S6: p-values obtained with the Tukey-Kramer (Nemenyi) post-hoc test corresponding to the E2-level pairwise analysis of the experimental groups. Values in red correspond to p<0.05

	CTR-F-1	CTR-F-2	CTR-M-1	CTR-M-2	E2-F-1	E2-F-2	E2-M-1
CTR-F-2	0.974						
CTR-M-1	1.000	1.000					
CTR-M-2	1.000	0.999	1.000				
E2-F-1	0.003	4E-05	0.147	0.025			
E2-F-2	0.008	1.41E-04	0.212	0.048	1.000		
E2-M-1	0.258	0.076	0.388	0.286	1.000	1.000	
E2-M-2	0.008	2.58E-04	0.133	0.031	1.000	1.000	1.000

Table S7: p-values obtained with the Tukey-Kramer (Nemenyi) post-hoc test corresponding to the HSI-value pairwise analysis of the experimental groups. Values in red correspond to p<0.05

	CTR-F-1	CTR-F-2	CTR-M-1	CTR-M-2	E2-F-1	E2-F-2	E2-M-1
CTR-F-2	0.999						
CTR-M-1	0.988	0.963					
CTR-M-2	0.864	0.953	0.645				
E2-F-1	0.009	0.042	0.052	0.942			
E2-F-2	1.610E-04	0.001	0.005	0.445	0.910		
E2-M-1	0.946	0.984	0.761	1.000	0.976	0.647	
E2-M-2	6.720E-04	0.003	0.006	0.416	0.874	1.000	0.596

Table S8: p-values obtained with the Tukey-Kramer (Nemenyi) post-hoc test corresponding to the Ca^2-level pairwise analysis of the experimental groups. Values in red correspond to p<0.05

	CTR-F-1	CTR-F-2	CTR-M-1	CTR-M-2	E2-F-1	E2-F-2	E2-M-1
CTR-F-2	0.940						
CTR-M-1	0.951	0.100					
CTR-M-2	0.985	1.000	1.000				
E2-F-1	3.4E-05	0.006	0.591	0.065			
E2-F-2	9.6E-05	0.010	0.615	0.083	1.000		
E2-M-1	0.493	0.911	0.998	0.944	0.977	0.979	
E2-M-2	0.493	0.641	0.992	0.805	0.897	0.913	1.000

Table S9: p-values obtained with the Tukey-Kramer (Nemenyi) post-hoc test corresponding to the P_i-value pairwise analysis of the experimental groups. Values in red correspond to p<0.05

	CTR-F-1	CTR-F-2	CTR-M-1	CTR-M-2	E2-F-1	E2-F-2	E2-M-1
CTR-F-2	1.000						
CTR-M-1	0.555	0.684					
CTR-M-2	0.979	0.996	0.968				
E2-F-1	0.193	0.350	1.000	0.966			
E2-F-2	0.019	0.049	1.000	0.651	0.988		
E2-M-1	1.000	1.000	0.930	1.000	0.932	0.655	
E2-M-2	0.601	0.768	1.000	0.997	1.000	0.966	0.985

In summary, except the Fulton's K condition factor, which presents a gender difference, the pertinent biometric and physiological parameters did not differ significantly between the groups from the two experiments. Hence, the results from both experiments were combined to increase the statistical power for detecting a possible oestrogenic modulation of T cell-related gene expression in males and female sea bass. Importantly, the parameters crucial for the experimental increase of E2-levels, *i.e.*, plasmatic E2-, Ca^{2+}- and P_i-levels as well as HSI were not different detected between the respective treatment groups of both experiments, *e.g.,* CTR-F-1 vs. CTR-F-2 (Tables S6-9) which confirmed that the experiments can be combined.

Table S10: p-value obtained with the Tukey-Kramer (Nemenyi) post-hoc test corresponding to E2-level pairwise analysis of the treatment group from both gender with experiment 1 and 2 combined. Values in red correspond to p<0.05

	CTR-F	CTR-M	E2-F
CTR-M	0.996		
E2-F	2.056E-08	2.76E-04	
E2-M	3.836E-05	0.003	1.000

Table S11: p-value obtained with the Tukey-Kramer (Nemenyi) post-hoc test corresponding to the HSI-value pairwise analysis of the treatment group from both gender with experiment 1 and 2 combined. Values in red correspond to p<0.05

	CTR-F	CTR-M	E2-F
CTR-M	9.744E-01		
E2-F	6.183E-07	0.006	
E2-M	3.007E-04	0.024	1.000

Table S12: p-value obtained with the Tukey-Kramer (Nemenyi) post-hoc test corresponding to the Ca^{2+}-level pairwise analysis of the treatment group from both gender with experiment 1 and 2 combined. Values in red correspond to p<0.05

	CTR-F	CTR-M	E2-F
CTR-M	0.851		
E2-F	2.152E-08	0.003	
E2-M	2.396E-02	0.371	0.356

Table S13: p-value obtained with the Tukey-Kramer (Nemenyi) post-hoc test corresponding to the Pi-level pairwise analysis of the treatment group from both gender with experiment 1 and 2 combined. Values in red correspond to p<0.05

	CTR-F	CTR-M	E2-F
CTR-M	0.319		
E2-F	5.590E-04	0.654	
E2-M	0.360	1.000	0.535

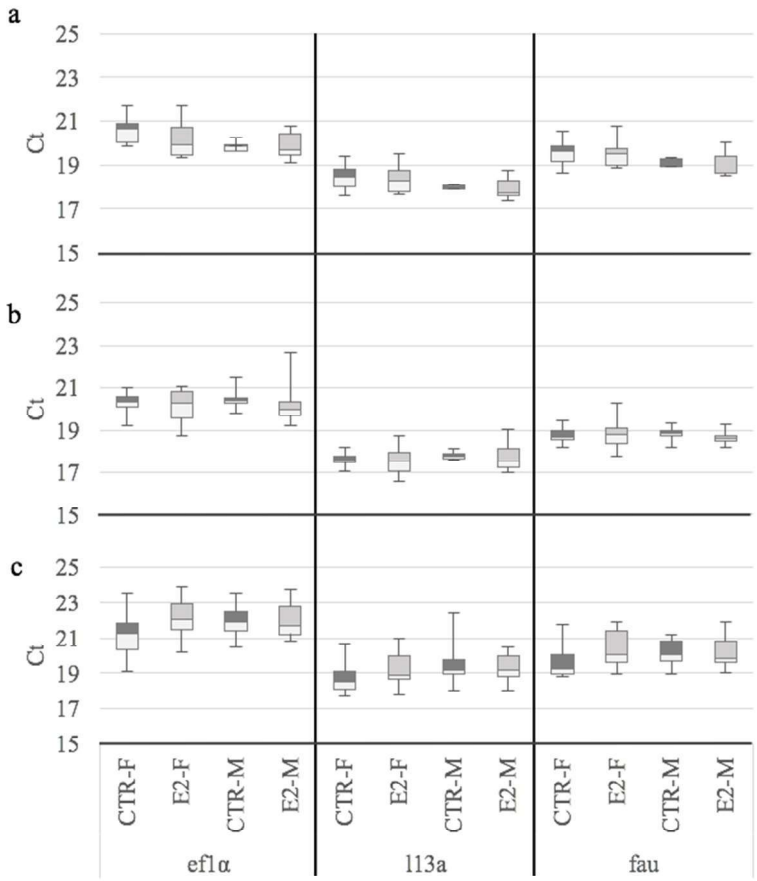

Figure S3: Cycle thresholds (Ct) for the reference genes assayed obtained in qPCR in three lymphoid organs of sea bass, Dicentrarchus labrax, in males (M) and females (F) of E2-exposed (E2) and control (CTR) fish for thymus (a), head-kidney (b) and spleen (c). Ct-values are represented by box-and-whisker plots with the median, 25 % and 75 % quartiles as well as extreme values depicted by the bars.

Table S14: Matrice of Spearman Rank Order correlation coefficients between the different variables measured in control females (A) and E2-injected females (B) in the thymus (T). For each correlation is the r, p and n values are shown (in this order).

A	*rag1*	*foxn1*	*aire*	*tcr-a-T*	*foxp3-T*	*tcrg-T*	*mhc2-T*	*pcna-T*	*Csp8-T*	*Csp9-T*
ikaros	0.626	**0.732**	0.0179	0.578	0.514	0.242	0.468	0.418	0.379	**0.707**
	0.0158	**0.00145**	0.944	0.0291	0.048	0.414	0.0873	0.117	0.158	**0.00278**
	14	**15**	15	14	15	13	14	15	15	**15**
rag1		0.516	0.13	0.665	0.451	0.0879	0.434	0.27	0.178	0.534
		0.056	0.648	0.0122	0.101	0.764	0.132	0.34	0.532	0.047
		14	14	13	14	13	13	14	14	14
foxn1			-0.129	0.587	**0.811**	-0.225	0.468	0.075	0.321	**0.757**
			0.639	0.0262	**0.2E-6**	0.447	0.0873	0.783	0.235	**0.000575**
			15	14	**15**	13	14	15	15	**15**
aire				-0.253	0.0821	-0.137	-0.2	-0.404	-0.239	-0.0786
				0.373	0.763	0.643	0.482	0.131	0.381	0.773
				14	15	13	14	15	15	15
tcra-T					0.358	0.011	0.64	0.235	0.116	0.64
					0.201	0.964	0.0131	0.407	0.682	0.0131
					14	13	14	14	14	14
foxp3-T						-0.412	0.385	-0.107	0.293	0.654
						0.154	0.167	0.695	0.281	0.00785
						13	14	15	15	15
tcrg-T							-0.137	0.159	-0.412	-0.187
							0.643	0.591	0.154	0.528
							13	13	13	13
mhc2-T								0.424	0.266	0.534
								0.125	0.348	0.047
								14	14	14
pcna-T									**0.711**	0.454
									0.00256	0.0861
									15	15
Csp8-T										0.682
										0.00471
										15

B	*rag1*	*foxn1*	*aire*	*tcr-a-T*	*foxp3-T*	*tcrg-T*	*mhc2-T*	*pcna-T*	*Csp8-T*	*Csp9-T*
ikaros	0.594	0.467	0.407	0.545	0.544	0.308	0.0275	0.313	0.456	0.335
	0.0387	0.102	0.16	0.0623	0.0517	0.295	0.921	0.286	0.111	0.252
	12	13	13	12	13	13	13	13	13	13
rag1		-0.21	0.301	0.164	0.364	-0.217	-0.035	-0.189	0.161	0.042
		0.498	0.329	0.614	0.233	0.484	0.904	0.542	0.603	0.886
		12	12	11	12	12	12	12	12	12
foxn1			0.0549	0.175	0.555	0.341	0.0879	0.33	0.516	0.67
			0.849	0.572	0.0464	0.244	0.764	0.261	0.067	0.0113
			13	12	13	13	13	13	13	13
aire				0.392	0.396	-0.126	0.313	-0.198	-0.011	0.198
				0.197	0.173	0.669	0.286	0.504	0.964	0.504
				12	13	13	13	13	13	13
tcra-T					0.196	-0.126	0.49	0.406	0.049	-0.189
					0.527	0.683	0.0998	0.181	0.869	0.542
					12	12	12	12	12	12
foxp3-T						-0.176	0.396	-0.115	0.72	0.643
						0.553	0.173	0.696	0.00473	0.0167
						13	13	13	13	13
tcrg-T							-0.368	0.0604	0.0769	0.363
							0.206	0.835	0.792	0.214
							13	13	13	13
mhc2-T								-0.121	-0.022	-0.011
								0.682	0.935	0.964
								13	13	13
pcna-T									0.187	-0.022
									0.528	0.935
									13	13
Csp8-T										0.681
										0.00948
										13

Table S15: Matrice of Spearman Rank Order correlation coefficients between the different variables measured in control females (A) and E2-injected females (B) in the head-kidney (HK). For each correlation is the r, p and n values are shown (in this order).

A	*foxp3-HK*	*tcrg-HK*	*mhc2-HK*	*pcna-HK*	*Csp8-HK*	*Csp9-HK*
tcra-HK	0.618	0.336	0.468	0.284	0.297	0.415
	0.0178	0.231	0.0873	0.316	0.293	0.134
	14	14	14	14	14	14
foxp3-HK		0.134	0.618	0.543	0.152	**0.758**
		0.637	0.0178	0.0429	0.594	**0.00102**
		14	14	14	14	**14**
tcrg-HK			0.38	0.292	-0.0418	0.187
			0.173	0.301	0.88	0.511
			14	14	14	14
mhc2-HK				**0.719**	0.134	0.345
				0.0032	0.637	0.219
				14	14	14
pcna-HK					0.341	0.464
					0.225	0.0907
					14	14
Csp8-HK						0.305
						0.279
						14

B	*foxp3-HK*	*tcrg-HK*	*mhc2-HK*	*pcna-HK*	*Csp8-HK*	*Csp9-HK*
tcra-HK	0.583	0.115	0.648	-0.0909	0.285	0.05
	0.0874	0.733	0.0377	0.785	0.404	0.878
	9	10	10	10	10	9
foxp3-HK		0.167	0.367	-0.0667	0.3	0.533
		0.643	0.308	0.844	0.407	0.124
		9	9	9	9	9
tcrg-HK			-0.136	0.3	0.0424	0.05
			0.673	0.353	0.892	0.878
			11	11	10	9
mhc2-HK				-0.0273	-0.0909	0.35
				0.924	0.785	0.331
				11	10	9
pcna-HK					-0.139	0.117
					0.681	0.742
					10	9
Csp8-HK						0.0833
						0.809
						9

Table S16: Matrice of Spearman Rank Order correlation coefficients between the different variables measured in control males (A) and E2-injected males (B) in the head-kidney (HK). For each correlation is the r, p and n values are shown (in this order).

A	*foxp3-HK*	*tcrg-HK*	*mhc2-HK*	*pcna-HK*	*Csp8-HK*	*Csp9-HK*
tcra-HK	0.6 0.0769 9	0.7 0.0301 9	0.533 0.124 9	-0.267 0.462 9	-0.4 0.264 9	0.75 0.0158 9
foxp3-HK		0.65 0.0501 9	0.433 0.223 9	0.117 0.742 9	0.25 0.491 9	**0.883** **0.2E-6** **9**
tcrg-HK			0.65 0.0501 9	0.35 0.331 9	-0.183 0.612 9	0.733 0.02 9
mhc2-HK				0.417 0.243 9	0.217 0.55 9	0.733 0.02 9
pcna-HK					0.333 0.356 9	0.233 0.52 9
Csp8-HK						0.167 0.643 9

B	*foxp3-HK*	*tcrg-HK*	*mhc2-HK*	*pcna-HK*	*Csp8-HK*	*Csp9-HK*
tcra-HK	0.382 0.233 11	0.394 0.243 10	**0.9** **0.2E-6** **11**	-0.127 0.693 11	-0.164 0.614 11	0.0727 0.818 11
foxp3-HK		0.588 0.0665 10	0.391 0.221 11	0.327 0.31 11	0.191 0.557 11	**0.782** **0.00285** **11**
tcrg-HK			0.43 0.199 10	0.212 0.535 10	-0.00606 0.973 10	0.527 0.107 10
cmh2-HK				-0.282 0.384 11	-0.136 0.673 11	0.0909 0.776 11
pcna-HK					0.473 0.132 11	0.518 0.0948 11
Csp8-HK						0.127 0.693 11

Table S17: Matrice of Spearman Rank Order correlation coefficients between the different variables measured in control females (A) and E2-injected females (B) in the spleen (S). For each correlation is the r, p and n values are shown (in this order).

A	*foxp3-S*	*tcrg-S*	*mhc2-S*	*pcna-S*	*Csp8-S*	*Csp9-S*
tcra-S	0.145 0.653 11	-0.145 0.653 11	0.0909 0.776 11	-0.2 0.559 10	-0.0182 0.946 10	-0.127 0.693 11
foxp3-S		0.622 0.0285 12	0.126 0.683 12	0.118 0.714 11	0.182 0.575 11	-0.021 0.939 12
tcrg-S			-0.0909 0.766 12	-0.382 0.233 11	0.0909 0.776 11	-0.0699 0.817 12
mhc2-S				-0.373 0.245 11	0.364 0.257 11	-0.517 0.0795 12
pcna-S					-0.479 0.148 10	0.582 0.0555 11
Csp8-S						-0.664 0.0234 11

B	*foxp3-S*	*tcrg-S*	*mhc2-S*	*pcna-S*	*Csp8-S*	*Csp9-S*
tcra-S	0.58 0.0446 12	0.627 0.0354 11	0.028 0.921 12	-0.497 0.0944 12	0.126 0.683 12	0.315 0.306 12
foxp3-S		0.709 0.0127 11	0.469 0.117 12	-0.035 0.904 12	0.0699 0.817 12	0.51 0.0843 12
tcrg-S			0.0818 0.797 11	0.00909 0.968 11	0.264 0.416 11	0.173 0.595 11
mhc2-S				0.119 0.699 12	-0.322 0.295 12	0.51 0.0843 12
pcna-S					0.0909 0.766 12	-0.105 0.733 12
Csp8-S						-0.559 0.0547 12

Table S18: Matrice of Spearman Rank Order correlation coefficients between the different variables measured in control males (A) and E2-injected males (B) in the spleen (S). For each correlation is the r, p and n values are shown (in this order).

A	foxp3-S	tcrg-S	mhc2-S	pcna-S	Csp8-S	Csp9-S
tcra-S	0.0909 0.785 10	0.515 0.116 10	0.0909 0.785 10	-0.286 0.46 8	-0.248 0.468 10	-0.2 0.559 10
foxp3-S		-0.103 0.759 10	0.261 0.446 10	-0.429 0.26 8	-0.588 0.0665 10	0.612 0.0537 10
tcrg-S			0.212 0.535 10	0.0952 0.794 8	0.188 0.583 10	-0.127 0.707 10
mhc2-S				0.119 0.749 8	0.103 0.759 10	0.0909 0.785 10
pcna-S					0.69 0.0474 8	-0.595 0.102 8
Csp8-S						-0.37 0.275 10

B	foxp3-S	tcrg-S	mhc2-S	pcna-S	Csp8-S	Csp9-S
tcra-S	0.75 0.0384 7	0.524 0.16 8	0.548 0.139 8	0.607 0.121 7	0.214 0.602 7	0.714 0.0545 7
foxp3-S		**0.929** **0.2E-6** **7**	**0.964** **0.2E-6** **7**	**0.964** **0.2E-6** **7**	0.679 0.0735 7	0.571 0.15 7
tcrg-S			**0.976** **0.2E-6** **8**	**0.964** **0.2E-6** **7**	0.607 0.121 7	0.643 0.0956 7
mhc2-S				**1** **0.2E-6** **7**	0.75 0.0384 7	0.5 0.217 7
pcna-S					0.75 0.0384 7	0.5 0.217 7
Csp8-S						-0.0357 0.905 7